SAND74-0391
Unlimited Release

Solar Total Energy Program Quarterly Report

July-September 1974

Solar Energy Projects Division 5712
Solar Energy Systems Division 5717

Prepared by Sandia Laboratories, Albuquerque, New Mexico 87115 and Livermore, California 94550 for the United States Atomic Energy Commission under Contract AT (29-1)-789

Printed December 1974

Sandia Laboratories
energy report

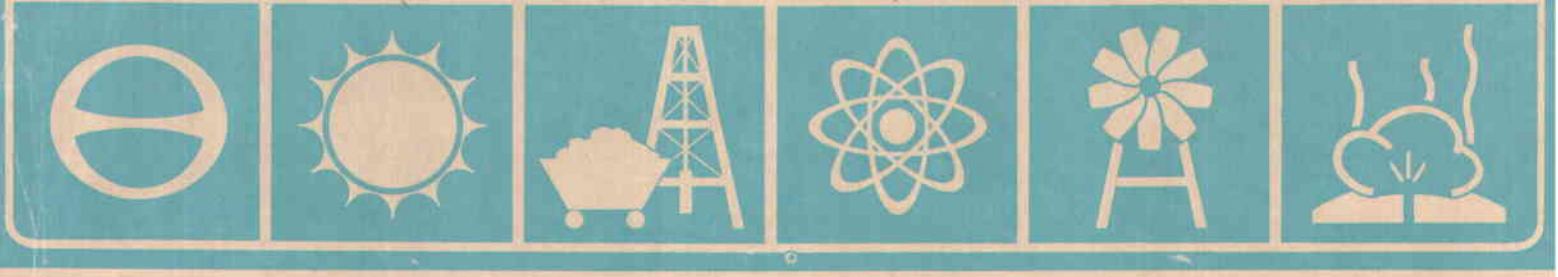

SF 2900-QQB(3-74)

Issued by Sandia Laboratories, operated for the United States Energy Research and Development Administration by Sandia Corporation.

SAND74-0391
Unlimited Release
Printed December 1974

SOLAR TOTAL ENERGY PROGRAM
QUARTERLY REPORT
July-September 1974

Prepared by J. A. Leonard
and
S. Thunborg
Solar Energy Projects Division 5712
Sandia Laboratories
Albuquerque, New Mexico 87115

ABSTRACT

This quarterly report describes the activities within Sandia Laboratories Solar Total Energy Program during the first quarter of fiscal year 1975. Included are the highlights of the quarter; descriptions of the system and its components, including some recent modifications to the baseline design; and the results of analyses and tests.

CONTENTS

ILLUSTRATIONS

SOLAR TOTAL ENERGY PROGRAM
QUARTERLY REPORT JULY-SEPTEMBER 1974

SECTION I

Introduction

The Solar Total Energy Program is the outgrowth of a series of exploratory system studies conducted at Sandia Laboratories since 1972, concerning potential uses of solar energy.

The studies have coalesced into the concept of a cascaded system in which solar energy collected at a central area is used to provide electrical power, heating, air conditioning, and hot water to a wide spectrum of users. A comprehensive hardware program designed to demonstrate one solar total energy concept is being conducted concurrently with systems analyses performed to investigate various additional means of implementing solar total energy concepts.

The primary objective of the Solar Total Energy Program is to determine and demonstrate the technical and economic feasibility of solar total energy. Additional objectives of the overall program are (1) to encourage private sector participation in the program and in the development of components for the system, (2) to determine those areas of research and development that offer the greatest payoffs, (3) to develop and validate a systems analysis computer program capable of evaluating the great number of possible combinations of total energy system configurations, and (4) to provide a system, prior to the pilot plant stage, sufficiently versatile to be used as an engineering evaluation center, or test bed, for further development of individual components or other solar energy systems.

The Solar Total Energy Program is a cooperative program which is being funded jointly by the Atomic Energy Commission and the National Science Foundation. Within this program, work is also being conducted to extend systems analyses to a widespread range of potential applications and systems concepts pursuant to a previously received NSF grant (No. AG-564). The progress of this work will also be reported herein.

The Solar Total Energy System, depicted in block diagram form in Figure 1 and as an artist's concept in Figure 2, will operate as follows. A working fluid is heated in the receiver tubes of the solar collectors by reflected and focused solar radiation. This fluid is pumped to the high-temperature storage tank. On a demand basis, fluid is extracted from this storage to the toluene boiler which produces superheated vapor to power the turbine/generator. The boiler can also be operated from a fossil-fuel-fired heater to insure continuity of operation during extended cloudy periods. Turbine

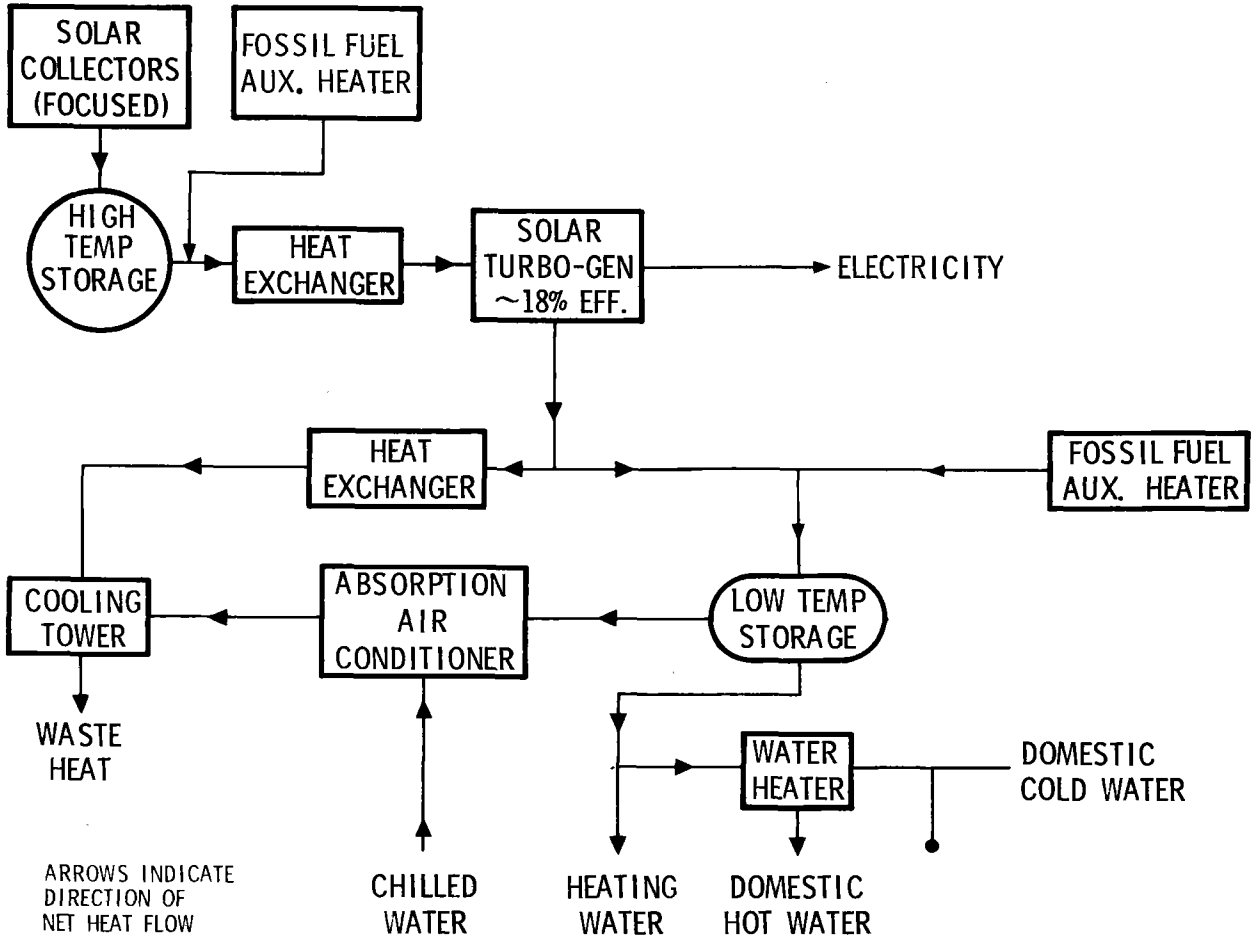

Solar Total Energy System simplified schematic

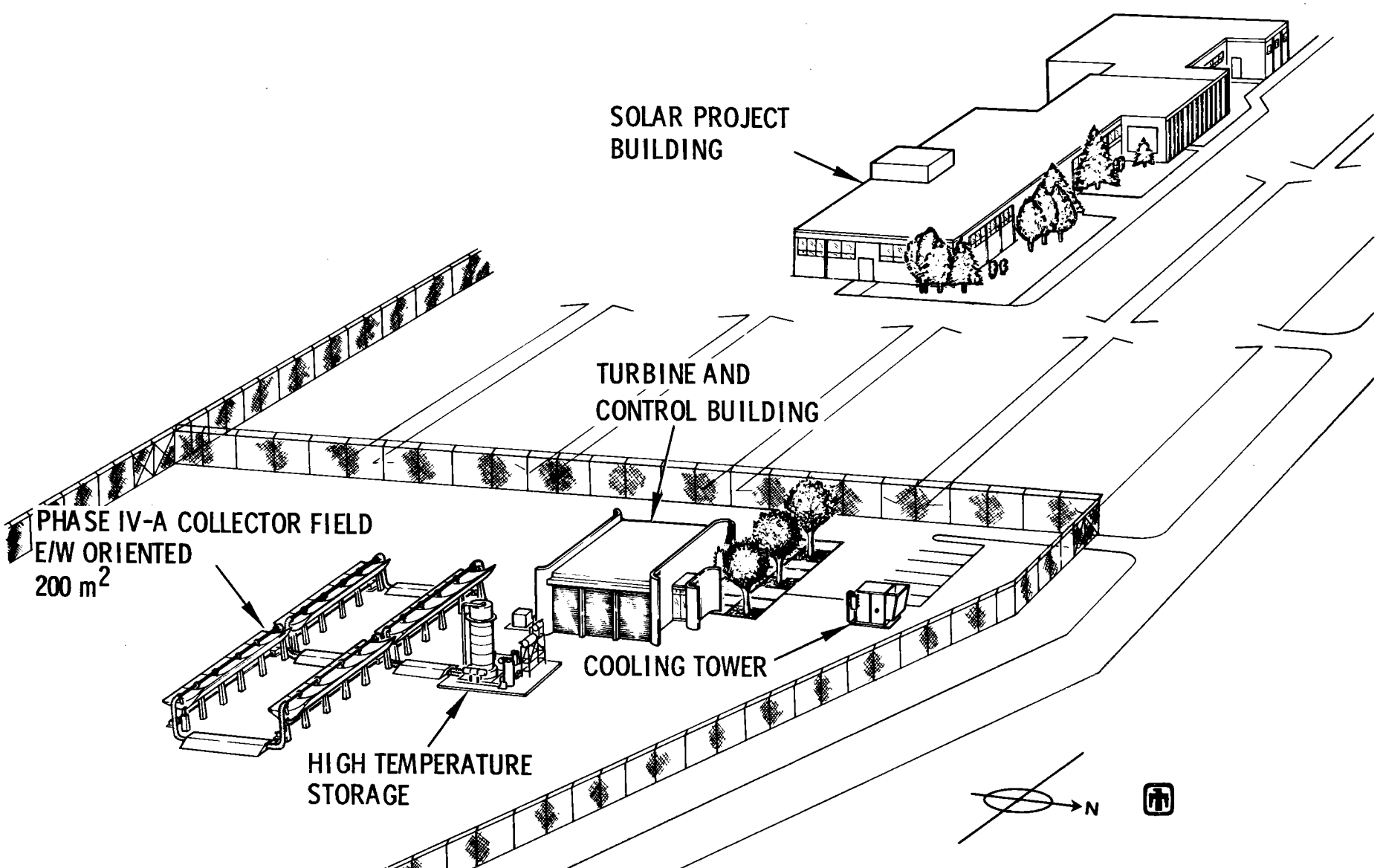

Figure 2. Solar Total Energy System

condenser coolant collected in the low-temperature fluid storage tank becomes the energy source for the low-temperature portion of the system. On a demand basis, fluid is extracted from low-temperature storage to power heating, air-conditioning, and hot-water-heating components.

The overall Solar Total Energy Program consists of seven phases of which the work being reported in this document is the beginning of Phase IV. The program, which was initiated in 1972 with background research and exploratory analysis, has progressed to the present hardware stage in which the test bed Solar Total Energy System is being built to provide power for an 1100 m^2 office building, the Solar Project Building. The program will conclude with the construction and operation of a solar total energy pilot plant expected to be achieved in cooperation with commercial interests.

Phases I, II, and III, which have emphasized preliminary studies and designs, have been completed. Phase IV-A began in July 1974. Phase IV-A is the pivotal phase in that it marks the transition from the analysis and design effort to the hardware and construction effort. Approximately 25 percent of the high-temperature solar-to-electric portion of the system is to be put into operation during this phase. Data collection in the high-temperature regime is of primary importance because little operating experience in this area has been accumulated.

During Phase IV-B, the remainder of the solar-to-electric components will be added, and the cascaded low-temperature portion of the system (heating, air conditioning, and hot water) will be installed.

Phase V will consist of operating the test bed under various conditions to gather and analyze engineering data which can provide a basis for the design of the pilot plant and for future solar energy systems. During this phase, the feasibility of powering and heating the Solar Project Building will be demonstrated.

Phases VI and VII will consist of the design, construction, and operation of a pilot commercial solar power plant. The overall Solar Total Energy Program plan and major milestones are illustrated in Figure 3.

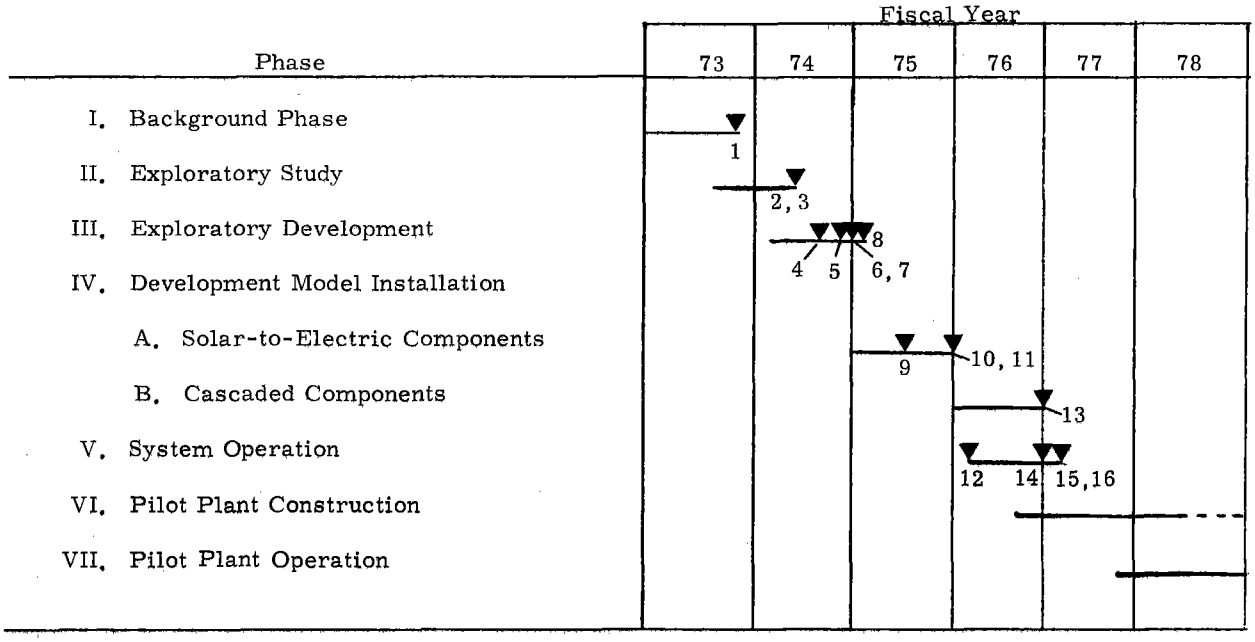

Milestones:

1. Completion of Phase I
2. Preliminary system design complete
3. Economic evaluation complete
4. Collector evaluation facility complete
5. System analysis program operational
6. Baseline system design complete
7. Phase IV-A proposal submitted
8. Phase IV-A supplementary proposal submitted
9. System analysis program loads profiles established
10. Partial collector field, storage, and turbine-generator test bed complete
11. Solar and weather input data established
12. Initial operation of partial Solar Total Energy test bed
13. Remainder of Solar Total Energy System completed
14. System analysis program refined and revalidated
15. Operation of complete Solar Total Energy System
16. Demonstration of Solar Project Building
17. Pilot plant designed
18. Pilot plant operational

Figure 3. Solar Total Energy Program schedule and milestones

SECTION II

Highlights

The following activities and milestones highlighted this reporting period:

- Baseline design of collector field changed to horizontal E/W orientation.
- Superheat cycle selected for turbine to improve storage efficiency.
- Fluid-flow analyses performed to optimize flow rates, receiver-tube plug diameter, and series/parallel collector arrangements.
- Work breakdown structure expanded to include technology support tasks.
- Fluid-flow transient analysis computer program, CNTROL, being used to develop control system strategy.
- Low cost reflector backing structure selected for baseline design.
- System analysis program, SOLSYS, extended to evaluate 1000-house community as well as Solar Total Energy Project.
- Installation of two 2.74- x 3.66-m, N/S, tilted parabolic collectors at collector evaluation facility initiated.
- Parabolic and flat plate collector performance data being measured at Collector Test Facility.

Reports and Presentations

The following reports and presentations have been completed in support of the Solar Total Energy Program during the reporting period.

Reports

1. Proposal for AEC/DAT, and the National Science Foundation Cooperative Support of Solar Total Energy Project Activities, Sandia Laboratories, Albuquerque, New Mexico, Solar Energy Projects Division 5712, SAND74-0141, July 1974.
2. W. P. Schimmel, The Solar Incidence Factor and Other Geometric Considerations of Solar Energy Collection, Sandia Laboratories, Albuquerque, New Mexico, SAND74-0026, July 1974.
3. T. D. Brumleve, Sensible Heat Storage in Liquids, Sandia Laboratories, Livermore, California, SLL-73-0263, July 1974.

4. W. H. McCulloch and G. W. Treadwell, Design Analysis of Asymmetric Solar Receivers, Sandia Laboratories, Albuquerque, New Mexico, SAND74-0124, August 1974.

5. J. A. Leonard and S. Thunborg, Solar Total Energy Program Quarterly Report, April-June 1974, Sandia Laboratories, Albuquerque, New Mexico, SAND74-0208, September 1974.

Presentations

1. R. P. Stromberg, Solar Energy, Albuquerque Sunport Optimists, July 3, 1974.

2. R. P. Stromberg, Sandia Solar Total Energy Program, ARPA Materials Research Council, La Jolla, California, July 8-10, 1074.

3. Solar Total Energy Project Staff (Divisions 5712 and 5717), Solar Total Energy Program Review, AEC Laboratories Program Review, Sandia Laboratories, Albuquerque, New Mexico, July 29, 1974.

4. R. H. Braasch, Solar Total Energy Program, EPRI Solar Program Planning Workshop, Palo Alto, California, August 12-15, 1974.

5. International Solar Energy Society, U. S. Sectional Annual Meeting, Fort Collins, Colorado, August 20-23, 1974.

   R. P. Stromberg, A Status Report on the Sandia Laboratories Solar Total Energy Program.

   L. G. Rainhart and W. P. Schimmel, Jr., Effect of Outdoor Aging on Acrylic Sheet.

   W. H. McCulloch and G. W. Treadwell, Design Analysis of Asymmetric Solar Receivers.

6. D. O. Lee and W. P. Schimmel, Jr., An Axial Temperature Differential Analysis of Linear Focused Collectors for Solar Power, 9th IECEC, San Francisco, California, August 26-30, 1974.

7. R. P. Stromberg, Sandia Solar Total Energy Program, NSF Solar Thermal Program Review, Denver, Colorado, September 23-25, 1974.

8. B. W. Marshall, Solar Energy Research at Sandia Laboratories, AIIE, Albuquerque Section, Albuquerque, New Mexico, September 25, 1974.

9. J. P. Abbin, Selection of a Low Temperature Energy Conversion System for Sandia's Solar Community Prototype, University of New Mexico, Mechanical Engineering Department Seminar, Albuquerque, New Mexico, September 30, 1974.

SECTION III

System Description and Status

Phase IV of the Solar Total Energy Program has been organized into a work breakdown structure of tasks and subtasks which are outlined below under Program Management. This section presents the detailed status of each program task.

Task 1 - Program Management

The work breakdown structure was expanded during this quarter to include the underlying technology development tasks which are conducted in support of the "hardware" tasks. The current task structure is as follows:

Work Breakdown Structure
Solar Total Energy Program, Phase IV-A

Task 1	Program Management
Task 2	System Management
2.1	System Engineering
2.2	System Analysis
Task 3	Collector Field
3.1	Reflectors and Structure
3.2	Receiver
3.3	Tracking and Drive System
3.4	Fluid Transfer System
3.5	Cooler
Task 4	High-Temperature Storage
Task 5	Turbine/Generator System
5.1	Boiler
5.2	Turbine
5.3	Rankine Loop Heater
5.4	Turbine Heat Exchanger
5.5	Cooling Tower
5.6	Load Bank
Task 6	Instrumentation and Control System
Task 7	Collector Test Facility
Task 8	Improved Data Base Compilation
8.1	System Load Profiles
8.2	Solar and Weather Input Data
8.3	Alternate T/E Systems

Task 9 Phase IV-B Supportive Energy Research

9.1 Collector Fabrication Development

9.2 Storage Technology

9.3 Theoretical Studies

Task 10 Coatings Evaluation

Task 11 Technology Utilization

A supplementary proposal (see Item 1, page 11, under Reports and Presentations) which incorporated these tasks and requested that Phase IV-A of the Solar Total Energy Program be jointly supported by the AEC, Division of Applied Technology, and NSF was prepared and submitted in July. The proposal was forwarded to Washington by AEC/ALO.

Task 2.1 - System Engineering

The system engineering efforts during this quarter resulted in five basic changes to the baseline design; two of these were of major significance. The significant changes were the adoption of a superheated cycle for the turbine and the use of E/W oriented collectors instead of N/S collectors. The other changes were (1) a reduced low-temperature storage capacity, (2) the introduction of a small buffer control tank between the collectors and the high-temperature storage, and (3) the elimination of a 20-percent excess collector area. Figure 4, which incorporates the above changes, presents the latest system schematic.

Superheated Cycle. The advantages of a superheated Rankine cycle for the Solar Total Energy Project were discussed in detail in the previous quarterly report. The point of this discussion was that while, generally, organic Rankine cycles are most efficient when the amount of superheat is minimized, the incorporation of small amounts of superheat into the cycle permits significant increases in the effectiveness of high-temperature storage by increasing the temperature drop of T-66 as it passes through the toluene boiler. In the Solar Total Energy Project herein, superheat also allows an increase in maximum cycle temperature without an increase in the T-66 heating fluid temperature. Table I summarizes the effect on cycle efficiency and temperature drop in storage of the previous saturated cycle and the present superheated cycle. The results are based on maintaining the same maximum temperature of the T-66 heating fluid and consequently of the collectors, i.e., 310°C.

TABLE I

Comparison of Superheated and Saturated Cycles

	Superheated Cycle 304°C (580°F) Max Cycle Temp		Saturated Cycle 288°C (550°F) Max Cycle Temp	
	Cycle Efficiency	Storage ΔT	Cycle Efficiency	Storage ΔT
Summer (200°F Condenser)	15.6%	72°C	15.6%	43°C
Winter (165°F Condenser)	17.7%	79°C	17.5%	44°C

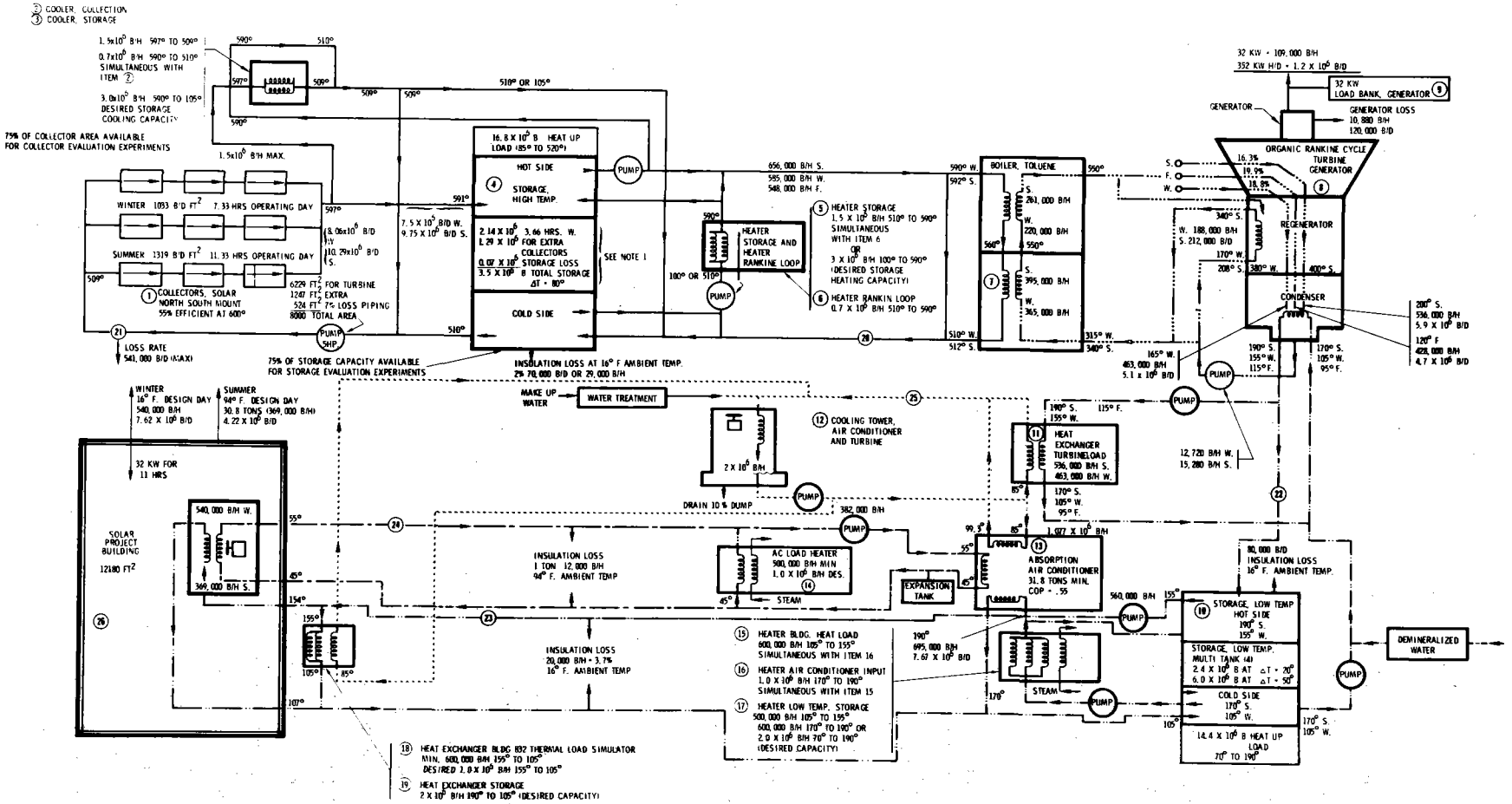

NOTES:

1. 1.29×10^8 EXTRA STORAGE WILL ALLOW FOR EXTRA STORAGE CAPACITY OF 2 HOURS IN WINTER AND 5 HOURS IN SUMMER.
2. ALL COMPONENTS AND PIPING IN THE GLYCOL/WATER LOOP SHOULD BE SIZED FOR GLYCOL/WATER MIXTURES. HOWEVER INITIALLY THE SYSTEM WILL BE OPERATED USING WATER ONLY.

S. = SUMMER OPERATION
W. = WINTER OPERATION
F. = MAX. EFF. OPERATION

CODE FLUID LOOPS

GLYCOL/WATER (SEE NOTE 2)
WATER, CHILLED
THERMINOL 66
TOLUENE
WATER, COOLING TOWER

COMPONENTS LIST

1. COLLECTORS, SOLAR
2. COOLER, COLLECTOR
3. COOLER, STORAGE
4. STORAGE, HIGH TEMP
5. HEATER, STORAGE
6. HEATER, RANKINE LOOP
7. BOILER, TOLUENE
8. ORGANIC RANKINE CYCLE TURBINE-GENERATOR
9. LOAD BANK, GENERATOR
10. STORAGE, LOW TEMP
11. HEAT EXCHANGER, TURBINE LOAD
12. COOLING TOWER, TURBINE AND/OR AIR CONDITIONER
13. ABSORPTION AIR CONDITIONER
14. AIR CONDITIONER LOAD HEATER
15. HEATER, BUILDING HEAT LOAD
16. HEATER, AIR COND. INPUT HEATER
17. HEATER, LOW TEMP STORAGE
18. HEAT EXCHANGER, BLDG. 832, THERMAL LOAD SIMULATOR
19. HEAT EXCHANGER, STORAGE
20. THERMINOL LOOP, STORAGE TO TURBINE
21. THERMINOL LOOP, COLLECTOR TO STORAGE
22. GLYCOL LOOP, TURBINE TO STORAGE
23. GLYCOL LOOP, STORAGE TO LOADS
24. CHILLED WATER LOOP
25. COOLING TOWER LOOP
26. BUILDING MODIFICATIONS
27. INSTRUMENTATION AND CONTROL

Figure 4. Solar Total Energy System schematic

As indicated by the larger storage ΔT of the superheated cycle and by the fact that storage size is proportional to storage ΔT, the use of this cycle allows the storage capacity for the superheated cycle to be reduced to only 56 percent of that required for the saturated cycle. In addition, a slight improvement in collector operating efficiency is obtained as a result of a decrease of 14°C of the average operating temperature of the collector.

E/W Oriented Collectors. A study was made to determine whether E/W or N/S tracking focused collectors should be used for the Solar Project Building. This study indicated that there would be no economic penalty associated with the use of E/W collectors and that there may be a substantial economic advantage (40 percent cheaper) to their use.

The results of the study are summarized in Table II.

TABLE II

Comparison of E/W versus N/S Collector Orientation

N/S			E/W	
Cost	Size	Component	Size	Cost
$52,450	487 m^2	Collector for load	658 m^2	$35,385-53,077
7,030	65 m^2	Collectors for pipe losses	27 m^2	1,440- 2,160
59,480	552 m^2	Total collector area	685 m^2	36,825-55,237
7,552	1,430,000 kJ	Storage capacity	2,090,000 kJ	11,000
5,195-10,340	317 m	Piping	83 m	1,365- 2,730
Free	1,746 m^2	Land	1,854 m^2	---
$72,227-$77,422		Total Cost		$49,190-$68,967

It should be noted that the advantage of E/W collectors over N/S tilted collectors comes primarily from a reduction in piping costs (piping and collectors for pipe losses) and potentially from a difference in the cost of E/W collectors over N/S collectors.

The results are not considered to be general; rather they are peculiar to the Solar Total Energy Project because of the specific design load profile. In essence, the design is based on meeting the steady 32-KW electrical load for 11 hours (7 AM to 6 PM). The building heating and cooling loads are then met from the energy available from the turbine condenser. The electricity is generated at 17.7-percent efficiency in the winter but at only 15.6-percent efficiency in the summer because of the need to increase the turbine condenser temperature to 88°C for the air-conditioner operation. Consequently, 13 percent more energy is required to meet the electrical loads in the summer than in the winter. Therefore, the study assumed that if more than 13 percent energy could be collected in the summer than the winter, this excess energy would not be used. For the loads of the Solar Project Building, this is a correct assumption; however, it severely penalizes N/S-type collectors because they are capable of collecting up to 50 percent more summer energy.

The following factors were considered in the evaluation of N/S versus E/W collectors for the Solar Project Building:

1. Effect on Required Collector Area. E/W daily output is less than N/S; therefore, more E/W collectors are required.
2. Effect on Required Storage. E/W collectors require more storage capacity for the constant load of the Solar Project Building.
3. Collector Area Required to Replace Pipe Losses. The E/W field required less collection piping; therefore, the total losses from the pipes are less, and consequently less collectors to replace these losses are required.
4. Cost of Piping System. An E/W collector field requires less pipeline length.
5. Cost of Land. E/W collectors require more collectors but have a better land utilization factor for a given shadowing loss than N/S.
6. End Loss Effects. The N/S collectors considered herein are fixed at 45 degrees and track about this axis daily. Consequently, they are subject to end losses throughout most of the year. This effect has been compensated for by the addition of end mirrors which are changed from one end to the other for summer and winter operations.
7. Incidence Angle Effects. E/W collectors are affected more than N/S collectors by the effect of incidence angle on reflectivity and absorption. The computer code predicting collector output incorporates these effects.

The economic data were based on estimated mass production costs for large systems. In that the purpose of the Solar Total Energy Program is to build a system representation of the large systems that will be required for total energy applications, the mass production costs were applied to the 32-KW system in order to insure an E/W versus N/S decision representative for large systems. The economic inputs were as follows:

Collectors:	N/S = $\frac{\$108}{m^2}$ ($\$10/ft^2$)
	E/W = \$54, \$67, and \$80/m^2
Storage:	\$4.75/MJ (\$5.00/KBTU) of Capacity (316°C maximum temperature)
Piping System:	\$16.00, \$24.00, and \$32.00/linear meter (\$10.00/ft)
Land:	0, \$2.70, and \$8.00/m^2 (\$0.75/ft^2)
	31.6% land utilization factor N/S
	36.9% land utilization factor E/W

The collector field being fabricated during Phase IV-A represents only 25 percent of the total field. Consequently, if performance data for E/W and N/S collectors can be obtained before the remaining 75 percent is constructed, the data can be used to determine which system should complete the field. Accurate performance data on both E/W and N/S collectors can be obtained if the building field utilizes E/W collectors and if the Collector Test Facility is simultaneously used to evaluate N/S collectors. The reverse is not necessarily true because of the technical and economic practicality of testing a long E/W collector on the test facility. For these reasons and because of the potential economic gain, the Solar Total Energy Project will utilize four rows of tracking E/W collectors. Each row will be 18.3 meters long and will be composed of five each 2.74- x 3.66-meter collectors. The collectors will be interconnected so that they can be operated 5, 10, or 20 in series. Simultaneously with the construction of the E/W field, performance testing utilizing the Collector Test Facility will be conducted with a 2.74- x 3.66-meter N/S collector.

Low-Temperature Storage. Systems analysis efforts with the SOLSYS Program have shown that the size of low-temperature storage can be substantially reduced if the building is not heated during the nighttime. This practice will be followed because the thermal mass of the building is such that the temperature drop occurring overnight can be easily made up in the morning without discomfort to the occupants.

Buffer Control Tank. The buffer control tank prevents the introduction of excessively cold or hot fluid to the storage tank and thereby prevents disruption of the thermoclime during startup operations. The need for and advantages of this tank are discussed more fully under "Instrumentation and Control."

Extra Collectors Eliminated. The baseline schematic of Figure 4 does not have a 20-percent excess collector area as the previous schematic did. The present schedule allows for construction of the field in two phases; therefore, adequate performance data can be obtained prior to construction of the full field. As a result, the immediate need for an excess area to cover contingencies can be eliminated.

Collector Field Layout. The layout of the Phase IV-A collector field has been completed. Site preparation is planned for the next quarter. Figure 5 is a plan view of the collector field as well as of the Turbine and Control Building and other major subassemblies of the Solar Total Energy System.

The collector field will consist of 20 parabolic trough collectors mounted horizontally with their longitudinal axes aligned in the E/W direction. The collectors will be bolted together in groups of five. Each of these groups will have a common tracking and drive system to maintain alignment with the sun throughout the day. Single axis tracking will be employed. The collectors will rotate about their E/W axis to keep the incident solar energy in the plane of symmetry of the parabolas.

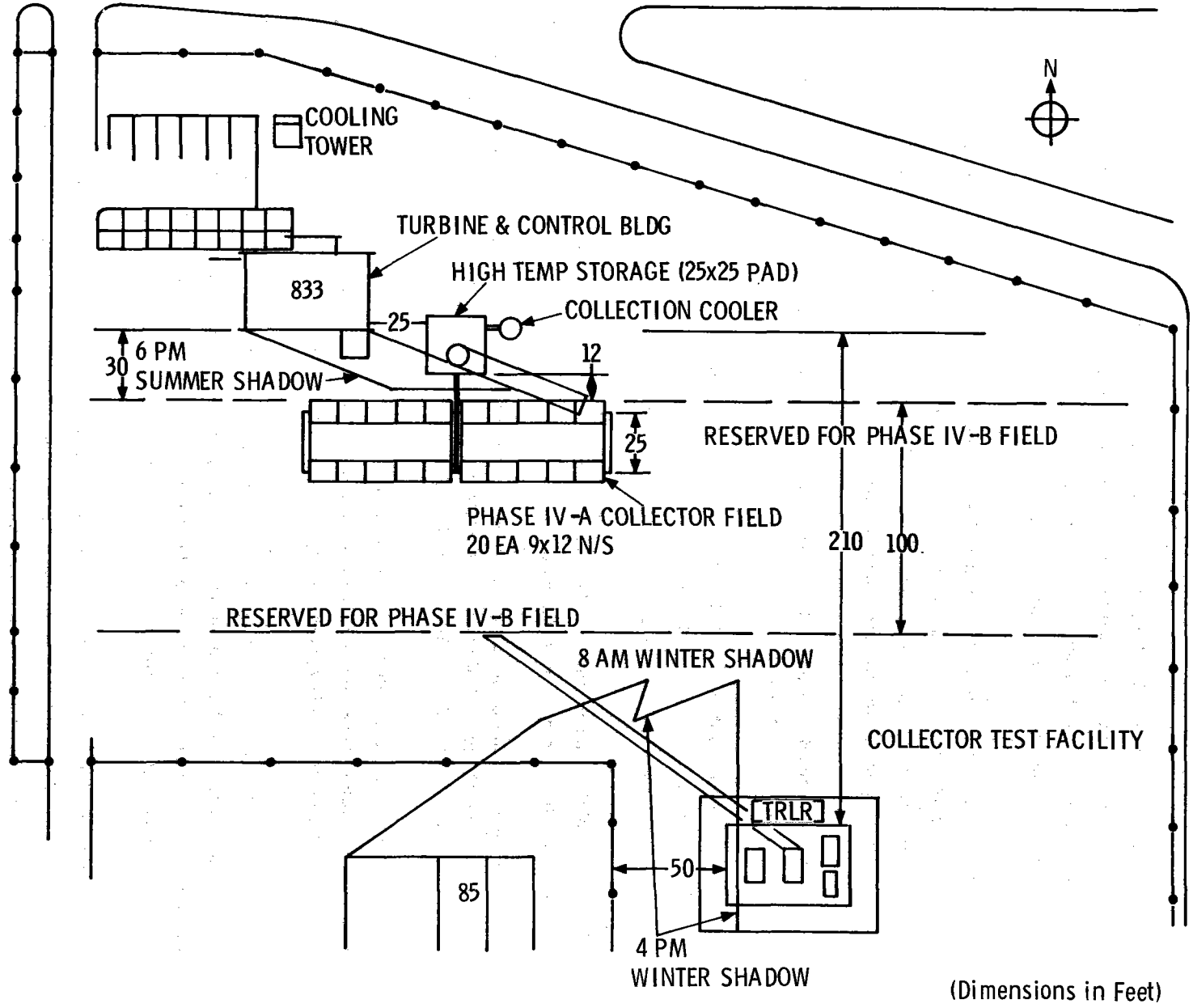

Figure 5. Solar total energy complex Phase IV-A layout

The receiver tubes in each group of five collectors will also be bolted together on flanges at 3.66-m (12 ft) intervals so that the working fluid will flow through the entire group without interruption.

The groups of five collectors will be arranged so that there are two E/W aligned rows of 10 collectors each. To minimize end losses at large solar incidence angles, the spacing between colinear rows will be kept as small as possible. To determine the optimum north and south spacing between each row of 10 collectors, the computer program SOLR was employed.

One of the features of SOLR is that given the spacing between rows of collectors it computes the effect on daily performance of mutual shadowing between collectors. A compromise must be decided upon between large row-to-row spacing which minimizes shadowing and the offsetting need to keep this spacing small to minimize thermal losses in the pipeline.

First, the spacing required for no shadowing at various times of the year was determined. The results were as follows:

Summer Solstice	4.6 m (15 feet)	center-to-center
Equinox	4.6 m	center-to-center
Winter Solstice	12.2 m	center-to-center

The winter solstice appeared to be the most critical; therefore, the spacing giving optimum performance at winter solstice was determined.

Figure 6 is a plot of net thermal energy versus collector center-to-center spacing. Here, the net thermal energy = total collected energy per day (including shadowing effects), minus thermal losses through the pipeline insulation.

The figure indicates that the optimum winter spacing is 7.6 m (25 feet), which is still sufficiently large to cause no mutual shadowing in the other three seasons. The winter loss caused by shadowing at this spacing is approximately 1 percent.

The high-temperature storage tank was located as close to the field and as close to the Turbine and Control Building as practical so that pipeline lengths and the associated thermal losses would be small. The cooling tower has been located as far north of the collector field as possible so that the plume of water vapor will not shadow the field.

The Collector Test Facility will eventually be moved from its present site to the location shown in Figure 5. It will be located far enough south of the collector field so that no shadowing interference will take place with the full field of collectors to be installed during Phase IV-B in FY 76.

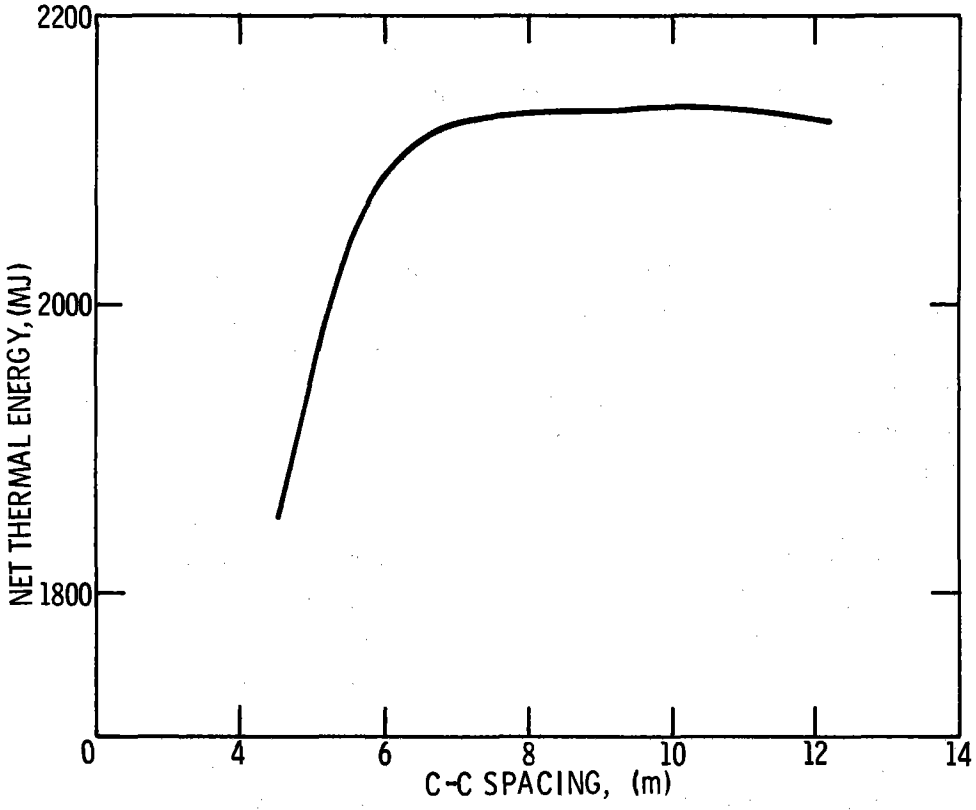

Figure 6. Net thermal energy versus collector spacing-winter solstice

Task 2.2 - Systems Analysis

Program SOLSYS. The Solar Energy Systems Simulation Program, SOLSYS, is a Fortran extended computer program which has been developed for analysis of energy systems. The program consists of four basic parts:

1. Main (executive) program
2. Component subroutine library
3. Information subroutine library
4. Control subroutine library

Executive Program

The executive program controls input, output, time iteration, and access to component, information, and control subroutines.

Component Subroutines

Component subroutines model components which receive a fluid, alter the fluid's temperature and pressure based on thermal and viscous interaction in the component, and pass the fluid to the next component. Components can be connected to form a fluid loop, and loops can be connected to form a complete system. Once a system is constructed, components can be easily interchanged or relocated and component parameters can be varied. Some of the components in the library are listed below:

Focusing collector	Flow dividers and junctions
Flat plate collector	Heat exchanger
Storage units	Cooling tower
Rankine cycle	Space heater
Pump	Air conditioner
Pipe	Hot water heater
Complete distribution system	Auxiliary furnace

Information Subroutines

Information subroutines provide necessary information to component subroutines. Some of these subroutines are listed below:

Solar position and intensity	Electric loads
Weather	Heating, air conditioning, and hot water loads

Control Subroutines

Control subroutines, which are used to control fluid temperatures in a circuit by controlling flow rate, are used to switch fluid flow. The value of a specified parameter, such as fluid temperature or storage volume, determines whether the fluid flow will be switched.

SOLSYS has been continuously improved and has been used for system and component performance studies during the past quarter. Because of the size and complexity of the program, modifications have been undertaken to provide increased computational efficiency. In addition, the new routines below have been incorporated to increase program versatility:

1. FLTPLTC, a flat plate collector modeling subroutine. This subroutine considers the following parameters:

   a. Orientation of the collector.

   b. Visible radiation transfer between the glass plates and from the collector surface.

   c. Conduction between glass plates and through back insulation material.

   d. Convection losses of the outer glass plate.

   e. Convection between the collector plate and working fluid.

2. HLOAD is a routine which computes the time-dependent loads of a single building. A detailed discussion of this program is presented under "Improved Data Base Compilation."

SOLSYS has been used to confirm the previously hand-calculated design of the Solar Total Energy System's collector area and high- and low-temperature storage capacity. Performance capabilities of the collector field were compared with the electrical, heating, and air-conditioning requirements of the Solar Project Building. SOLSYS output confirmed the system design very closely except for low-temperature storage which will be almost triple the size computed by SOLSYS. This is a consequence of heating and cooling the building only between the hours of 7:00 AM and 6:00 PM. The excess low-temperature storage will be retained to maintain system flexibility in the evaluation of other concepts where nighttime heating or daytime cooling is required.

Economic Studies

A computer subroutine is being used for making economic comparisons between alternative subroutines within the system or for providing a starting point for comparisons with other systems. The economic evaluations are based on the concepts underlying revenue requirement techniques. This technique takes into consideration the need for an adequate return on investment as well as the items considered as costs in the usual accounting determinations. The methodology for the calculation of annual revenue requirements is based on formulas derived from Professors Grant and Ireson* and on information obtained from the planning organization at Western Electric Company.

*Eugene L. Grant and W. Grant Ireson, Principles of Engineering Economy, Ronald Press Company, New York, 1964.

Figure 7 shows a diagram that summarizes the subroutine. The output is a figure referred to as the annual revenue requirement, which is the average amount that must be received each year to cover the economic cost of the project under consideration. In the case of such non-depreciable assets, as land and working capital, only the cost of money used for their acquisition is required. The value of these items is assumed to remain in the business, and additional cash outlays are not required. In the case of depreciable assets and future costs, a recovery factor is applied that takes into account the need to recover cash outlays as well as provide a return on money invested.

The left-hand column of Figure 7 indicates the various types of costs that must be estimated. Separate estimates are made for each component of the system. These estimates do not necessarily include all type of costs. For example, fuel costs might not be associated with hot water distribution, and general expenses would be included only in a total system. It should also be noted that estimates for buildings and equipment include interest paid during construction.

With respect to future costs, operating costs and maintenance are shown separately because operating costs are assumed to be at a level rate, except for inflation. Maintenance costs, on the other hand, might fluctuate with the lives of various types of equipment. Fuel is shown separately, because it is expected that fuel costs will increase regardless of inflationary pressures. General expenses are shown separately because they apply only to a full system and because it is anticipated that they will be subject to a separate escalation factor. Such items as property taxes and insurance should not fluctuate with the general economy.

An examination of literature available at the University of New Mexico's Bureau of Business Research indicates that economists cannot agree on the rate of inflation for any extended future period. For this reason, the computer program is written to allow the insertion of different escalation rates; as a result, the effect of a variety of rates can be determined.

In that the economic analysis encompasses expenditures at different times, the earning potential of money must be recognized. Therefore, expenditures through some period of time may be brought to an equivalent basis for comparison purposes by computing their present values. The formula for this is

$$PV = \frac{1}{(1 + i)^n} ,$$

where i = interest rate and n = number of interest periods. Here again, the computer program allows for inserting various interest rates for study purposes.

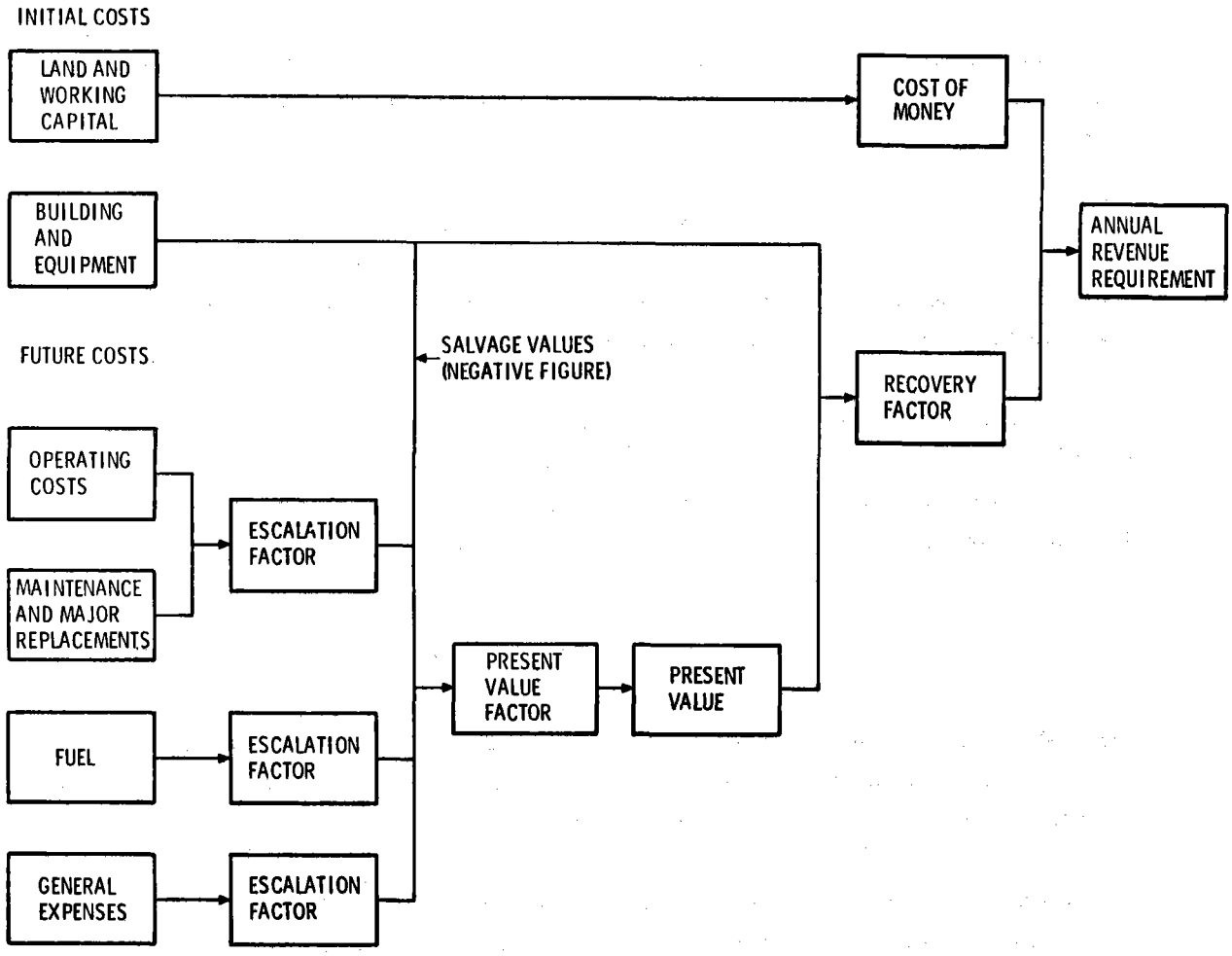

Figure 7. Economic subroutine diagram

The calculations explained so far ignore the effect of income taxes and possible variations in the methods of financing. Private investors would wish a reasonable return on investments after taxes, while income from borrowed capital would be taxable only to the extent that it exceeded interest paid. Also, any profit after taxes on borrowed capital increases earnings for the owners. Therefore, the mix in the source of capital (common stock, retained earnings, or bonds) has an effect on the revenue that must be received. In other words, the rate of return, or cost of money, must cover interest charges, taxes, and the profit desired by the owners.

The rate may be calculated with the analysis program on the basis of a variety of rates of return. Assuming that income taxes are 50 percent, the formula for calculating the pretax rate of return is

$$R = \frac{PS}{0.5} + B(1 - S) \quad ,$$

where P = the desired profit rate, S = the common-stock holders' percentage of the proposed total investment, and B = the cost of borrowed capital.

The annual revenue requirement for nondepreciable assets is the product of the rate derived above and the total value of such assets. In the case of all other expenditures, the money spent must be recovered or provided; therefore, the factor applied must take this into account as well as the cost of money. The formula for calculating this recovery (annuity) factor is

$$RF = \frac{i(1 + i)^n}{(1 + i)^n - 1} \quad .$$

The total annual revenue requirement is the requirement for nondepreciable assets plus the product of the recovery factor times all other expenditures. As is true for other items, the program will allow for substituting various interest rates and profit requirements in the calculations.

Economic comparisons between alternative components within the system can be made with this program. However, present differences in estimated costs for component parts make the results of the computation highly speculative.

A simplification of the cost analysis program has been prepared to calculate a level annual revenue requirement for individual homes for comparison to the Solar Total Energy System's annual revenue requirement. This calculation is needed to make a meaningful comparison of the essentially different types of expenses. Comparison of the level annual revenue requirement of the solar system, including the effects of inflation, to today's energy costs for a home would be incorrrect; future cost increases in energy for the homes must be considered. Results of such a single home are given below.

Based on present-day fuel prices (1974) and approximate hot water, electric, heating, and cooling demands of a single 140-m^2 (1500 ft^2) home, a one-home fossil fuel system in Albuquerque, NM, will cost $383.22 to operate in 1974.

This number was based on the following demands and prices:

Heating Demand:	107 GJ/yr	(102 MBTU/yr)
Cooling Demand:	3.2 GJ/yr	(900 KWh/yr)
Electric Demand:	27 GJ/yr	(7580 KWh/yr)
Hot Water Demand:	29 GJ/yr	(28.4 MBTU/yr)
Fuel Cost:	$0.93/GJ	($0.99/MBTU)
Electric Cost:	$6.9/GJ	($0.025/KWh)

Assuming a significant increase in fuel prices over the next 30 years associated with the conflict between supply and demand and an increase in operating costs resulting from inflation, the annual revenue requirement necessary for a household to supply its energy needs will become larger. For an inflation rate of 3-1/2 percent per year and a fuel cost inflation rate of 7 percent (these parameters are reasonably arbitrary and may be varied), 15 years from now $1271.80 will be required to purchase the same amount of energy that will cost $5041.73 in 30 years.

The total energy costs for the household over the next 30 years come to $53,914.21, which represents a present value of $10,793.38 at an interest rate of 9 percent. In other words, $10,793.38 placed in a bank account today at 9 percent interest would generate enough money over the next 30 years to meet all of the household's energy costs. If the household desired to equalize its payments over 30 years, the uniform yearly payment necessary to generate an amount equivalent to $53,914.21 would be $1050.59 each year for 30 years.

The number $1050.59 is the level annual revenue requirement for this one-home fossil fuel system. This figure is finally arrived at by applying a capital recovery factor to the present value of $10,793.38.

Use of other estimates for the increase in fuel costs will produce different results. Table III presents the results of some other calculations.

TABLE III

Some Estimates of Increases in Fuel Costs

	Fossil Fuel Price Increase*				
	1	2	3	4	5
Levelized Costs for Normal Home, $/yr	979	994	992	890	744

*
1. 40% for 2 yrs, 2% for 28 yrs
2. 15% for 5 yrs, 3% for 25 yrs
3. 7% for 20 yrs, 3% for 10 yrs
4. 7.5% for 12 yrs, 2% for 18 yrs
5. 3.75% for 30 yrs

Task 3.1 - Reflectors and Structure

The basic design of the parabolic trough reflector (Figure 8) is 3.66 m (12 feet) long and 2.74 m (9 feet) wide from rim to rim with a 92.4-degree rim angle and a focal length of 65.8 cm (25.9 inches). The reflector assembly consists of four panels faced with a highly reflective surface and mounted on a framework which in turn is mounted on trunnions atop steel and concrete pylons.* The individual panels are 1.8 cm (0.7 inch) thick. Four of these parabolic panels form the basic 2.74- x 3.66-m reflector unit.

The framework on which the four panels are mounted consists of five ribs running across the parabola and nominally spaced at 91 cm (3 feet) to provide support at each panel edge. The ribs at each end are inset to provide space for the mounting trunnions and the drive mechanism.

The longitudinal members of the framwork are steel or aluminum tubes or I-beams which provide the required structural support for high wind loads. These beams are welded to end plates which provide a means of attaching the ribs, the drive mechanism, the trunnions, and the receiver tube support structure.
receiver tube support structure.

The entire collector assembly will be supported at each end by a trunnion atop a concrete and steel pylon at a height of about two meters to provide ground clearnce so that the collector can be rotated freely about its longitudinal axis. A tracking and drive system (described later) will rotate the collector throughout the day to the proper attitude to keep the incident solar energy parallel to the plane of symmetry of the parabola.

As described earlier, the collector field to be installed during Phase IV-A will consist of 20 of the 2.74- x 3.66-m collectors arrayed in four rows of five collectors. Each set of five collectors will be "slaved" to rotate in unison; this will be accomplished by fastening their end plates together. A support pylon will be located every 3.66 meters under the interface between adjacent collectors.

The reflector back panel design has been developed with the support of Sandia's Composite Materials Development Division whose personnel have investigated numerous candidate back panel materials including laminated structures, stressed-skin sandwich structures with honeycomb cores and fiberglass/epoxy or polyester skins, and ribbed fiberglass/polyester structures with either fiberglass mat or sprayed-up chopped fiberglass roving.

A variety of small parabolas have been fabricated to evaluate these techniques, and two full-size 2.74- x 3.66-m ribbed fiberglass mat reflectors have been built and will soon go into performance testing.

---

*The material and fabrication details of the baseline panels are withheld due to patent considerations.

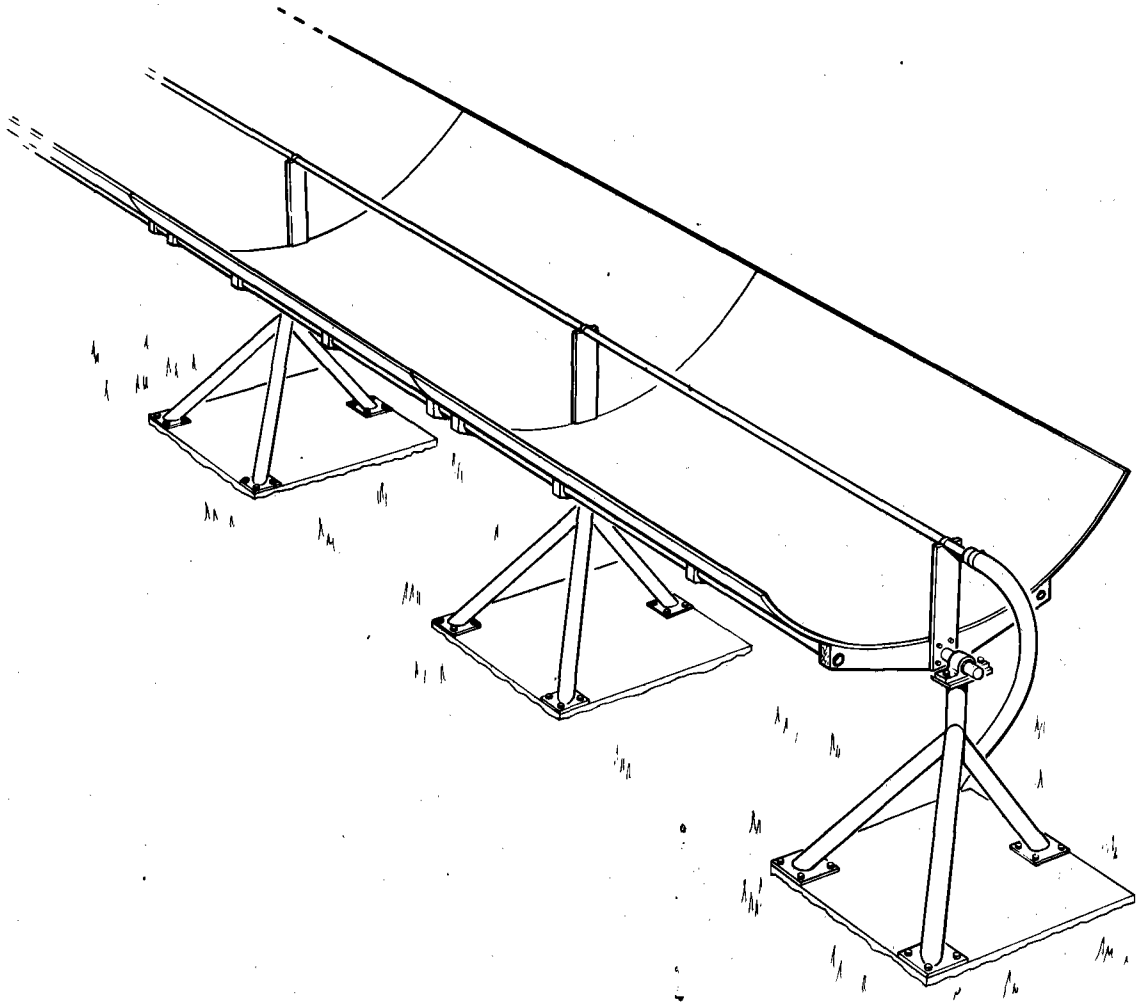

Figure 8. Basic design of the parabolic trough reflector

The most attractive concept to date has been verified by fabricating units 17 x 38 cm (7 x 15 inches) and 60 x 120 cm (2 x 4 feet) to contour over male molds. Polyester resin was used for the adhesive/impregnant in fabricating several units of both sizes.

The leading contender for the reflective surface has been Alzak, Alcoa's lighting sheet reflector, primarily because of its excellent long-term environmental capability and because of an advertised specular reflectance of 0.78 to 0.83. Alzak's availability in 0.64-mm (0.025-inch) sheet makes it convenient to use in reflector designs. However, investigations of other reflective materials are continuing. These investigations are reported in greater detail under "Collector Fabrication Development."

Task 3.2 - Receiver

The preliminary design of the receiver tube for the E/W Phase IV-A collector field has been completed. In cross-section (Figure 9), the receiver tube assembly consists of an evacuated glass envelope, enclosing the receiver tube itself, and a flow restrictor.

The glass envelope is 58.6 mm (2.3 inches) in diameter and 2.29 mm (0.090 inch) thick. Glass is used since it is transparent to the visible wavelengths, but opaque to the infrared radiation occurring as a result of receiver tube solar heating. The evacuated annulus within the glass envelope has a width of 6.35 mm (0.25 inch). Performance tests are being conducted at the Collector Test Facility to determine the level of vacuum which must be maintained for low heat transfer. Data presented by Saul, Dushman, and Lafferty* suggest that the air pressure within the annulus should be less than 10 mm Hg. If necessary, a fitting will be incorporated in the receiver tube design so that the vacuum can be periodically maintained.

The receiver tube which is 41.3 mm (1.625 inches) in diameter has a high absorptance, low emittance selective coating. As shown in Figure 9, the receiver tube angular size is 1-3/4 degrees. This angle includes the solar angle and assumed tracking and mirror slope errors. In addition, the assumption is made that photons striking at an angle greater than 60 degrees are reflected rather than absorbed; the tube diameter is inflated to preclude that event.

Because the thermal losses from the receiver tube are proportional to its surface area, it is important to minimize the diameter of the tube and still intercept all the focused solar energy from the reflector. This implies that the reflector rim-to-focus distance must be minimized for any given aperture. A study conducted by McCulloch and Treadwell** shows that these conditions are best satisfied by a collector with a 90-degree rim angle as shown in (Figure 10).

---

*Saul, Dushman, and Lafferty, Scientific Foundations of Vacuum Technique, John Wiley and Sons, 1962.

**W. H. McCulloch and G. W. Treadwell, Design Analysis of Asymmetric Solar Receivers, Sandia Laboratories, Albuquerque, NM, SAND74-0208, September 1974.

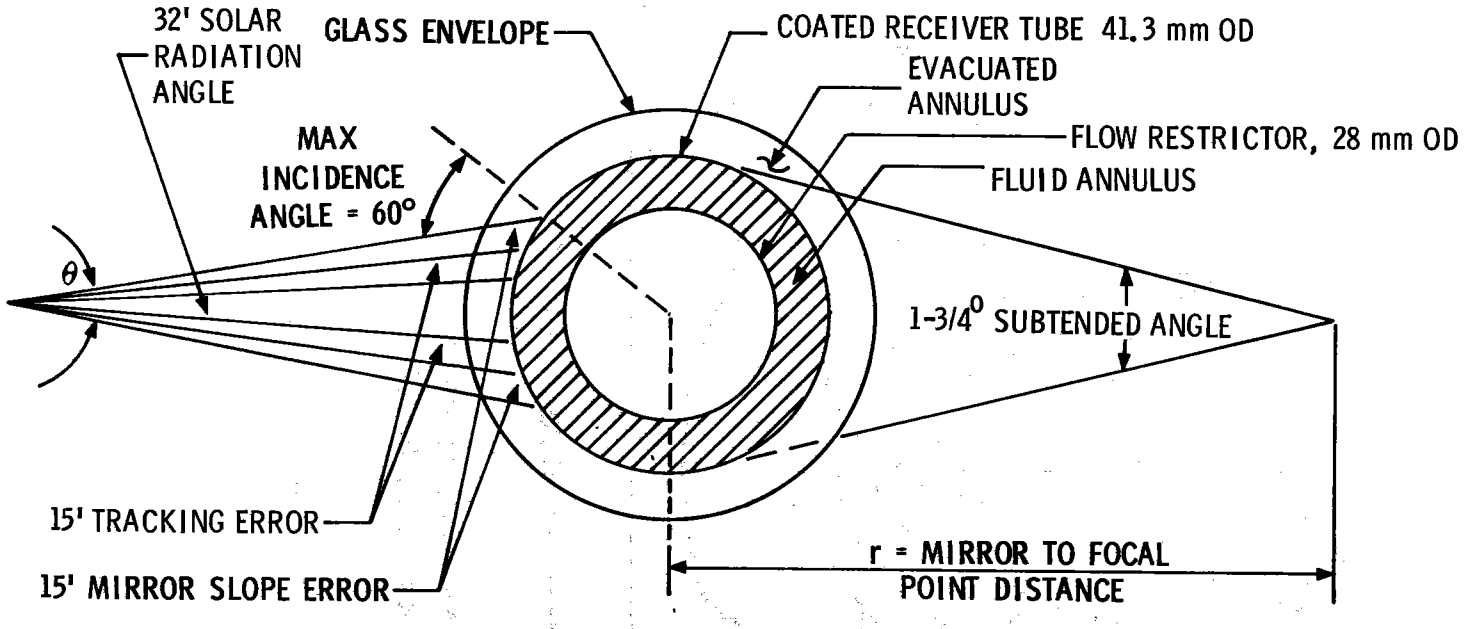

THERMAL LOSSES PROPORTIONAL TO RECEIVER TUBE DIAMETER

$$\text{RECEIVER TUBE DIAMETER} = \frac{2r \sin \theta_{1/2}}{\sin 60^\circ \sin (\text{RIM ANGLE})}$$

Receiver tube assembly cross section

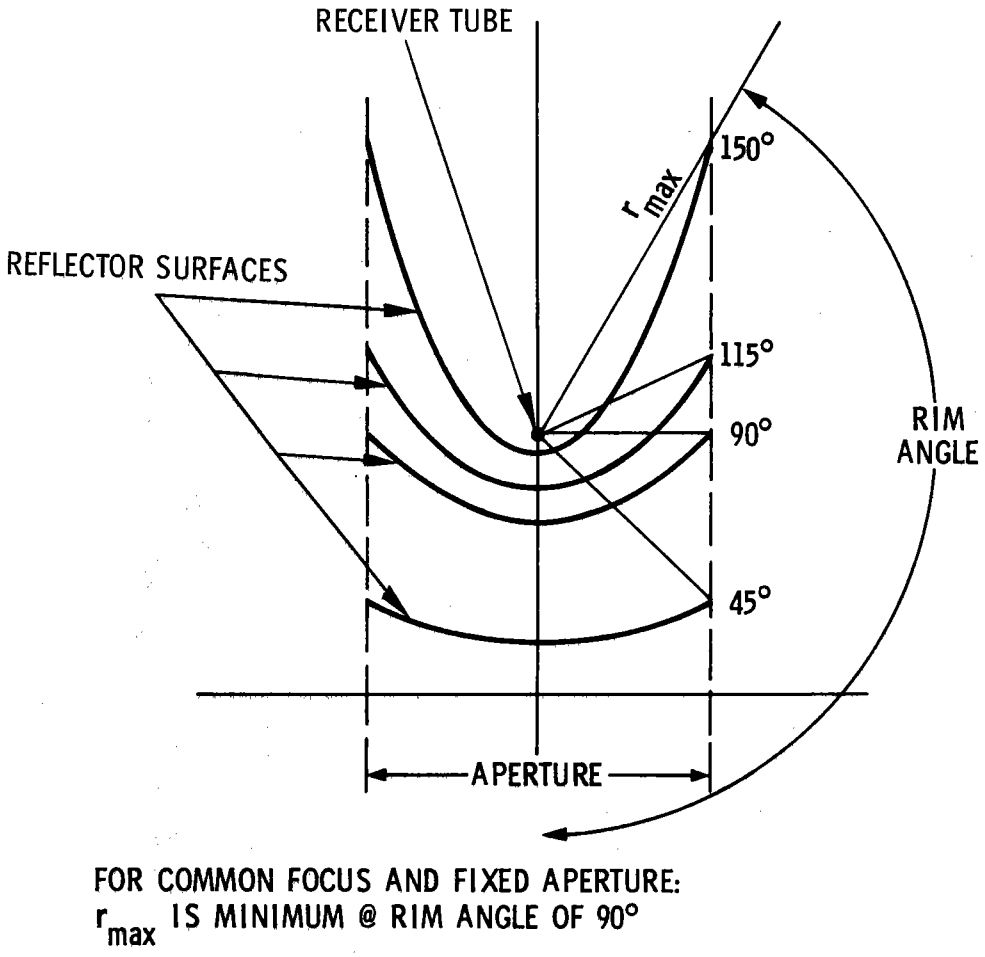

Figure 10. Collector rim angle

Numerical analyses were also conducted to consider the alternative of insulating the back surface of the receiver tube to determine whether different rim angles, which result in larger receiver tube diameters, could result in lower losses than a 90-degree rim angle. The results of that study corroborate the 90-degree rim angle.

The flow restrictor, or plug, has been incorporated to increase flow velocity and to minimize the radial temperature gradient in the fluid.

The radial temperature gradient (ΔT) at a given cross-section within a receiver tube is defined as the temperature difference between the inner surface of the receiver tube wall and the bulk fluid temperature. Because permanent damage to the T-66 will occur at excessive temperatures, the radial ΔT must be carefully controlled. The radial ΔT at the point of maximum receiver tube and bulk fluid temperature must be predicted under all operating conditions. The radial ΔT is computed as follows:

$$\text{Radial } \Delta T = \frac{Q}{hA} \quad ,$$

where Q = heat absorbed by receiver tube per unit length of collector, J/m - s

A = inner surface area of receiver tube per unit length, m

h = film coefficient on inner surface of receiver tube, J/m^2 - s - °C.

Figure 11 is a plot of radial ΔT versus flow rate for receiver tubes both with and without plugs. It indicates how the radial ΔT can get very large at low flow rates. In addition, the effects of adding plugs to the receiver tube are shown. The figure also implies that for a given bulk fluid temperature the receiver tube wall temperature will drop as plugs are added and the flow rate will increase. This drop in tube temperature results in decreased radiation losses and increased overall collector efficiency.

Other strategies are being considered for determining receiver tube size and shape. One is to determine, analytically and experimentally, the distribution of energy received from the reflector. If, for example, the reflected energy from the extreme edges of a reflector is small, the receiver tube may be decreased in diameter with little loss in incoming energy but large reductions of thermal losses. Once this energy distribution is known, it is possible that the receiver tube can be changed in shape for thermal loss reduction. For example, a triangular shape, which has less surface area than a circumscribed circular shape, could be oriented to improve incident angle effects.

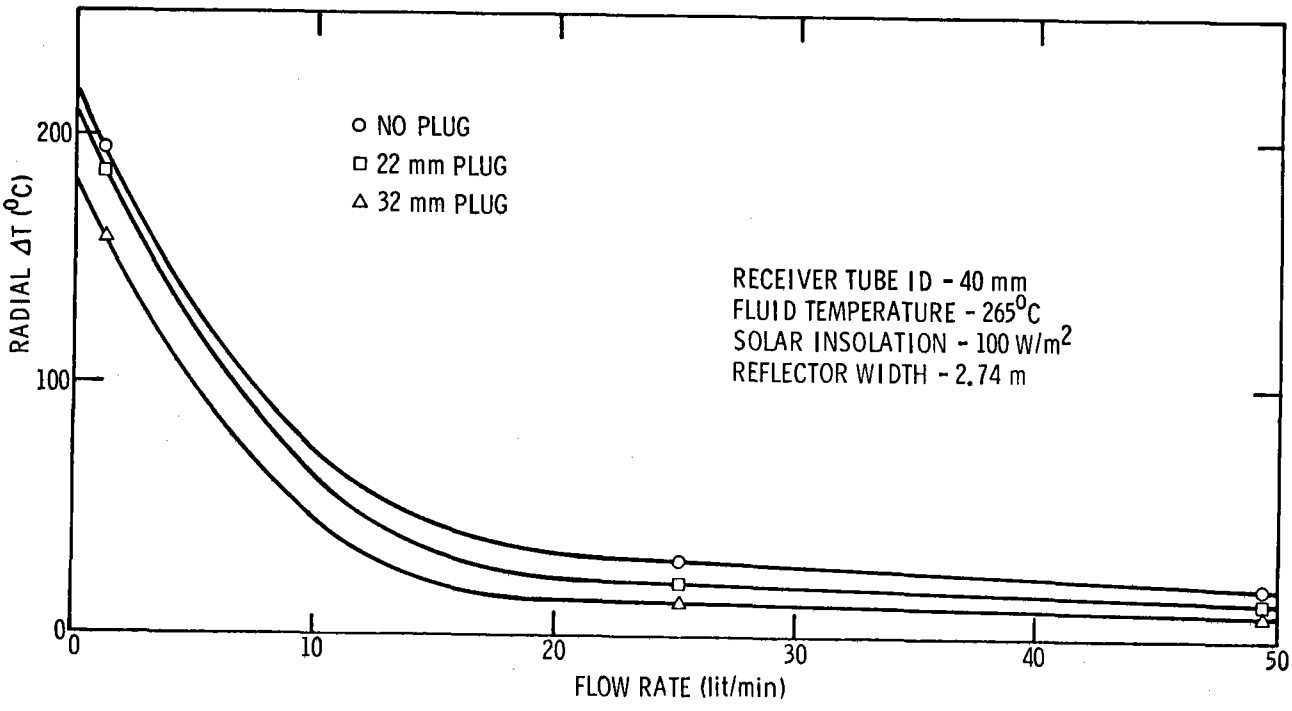

Figure 11. Radial ΔT versus flow rate

Task 3.3 - Tracking and Drive System

System Requirements. Tracking and drive systems are being developed for both N/S oriented and E/W oriented collectors. The requirements are similar, but the first system being developed is for the two tilted N/S collectors being installed at the Collector Test Facility. The detailed descriptions below apply primarily to the N/S tracking and control system. The design criteria are as follows:

- Maximum tracking error of 0.1 degree.
- The system must track both forward and backward.
- The system must have a minimum acquisition angle of 150 degrees.
- The system must have an automatic track mode during loss of lock (primarily for N/S).
- The system must be capable of intermittent operation with settable period.
- The system must be capable of defocusing a given amount on preset command.
- The gears and motor should be selected for fast return of collector.
- The system must interface with the HP2100 computer.

Drive System. The drive system consists of a 1/6-HP, DC, permanent-magnet, 137-volt motor which turns at 10,000 rpm into an integral 10:1 worm gear reduction box. This output is further reduced by a factor of 100:1 by a chain-drive sprocket. The driven sprocket is fixed to the collector end plate, and the diameter is such that an additional 14:1 speed reduction is effected. Thus, at full speed, the motor could drive the collector through 180 degrees in 42 seconds.

In the Phase IV-A collector field, one motor will be used for each row of five "slaved" collectors.

The period of intermittent operation will initially be set at 12 seconds. The Earth rotates through an arc of about 0.05 degree in 12 seconds; however, relative to a horizontal E/W collector, this rate varies throughout the day and is usually much less than 0.05 degree every 12 seconds. In Figure 12, which is a plot of reflector tracking angle throughout the day for three different seasons of the year, the slope of the tracking angle curve is the rate of track. Through the middle of the day, say from 9 A.M. to 3 P.M., the rate is nearly zero, and the tracking update period might be lengthened considerably. This is an additional, although minor, advantage of the E/W orientation.

For a continuously running, 1/6-HP motor, the 8-hour power usage would be

$$(0.75A)(137V) = \times 28,800 \text{ seconds} \approx 2,966,400 \text{ watt-seconds.}$$

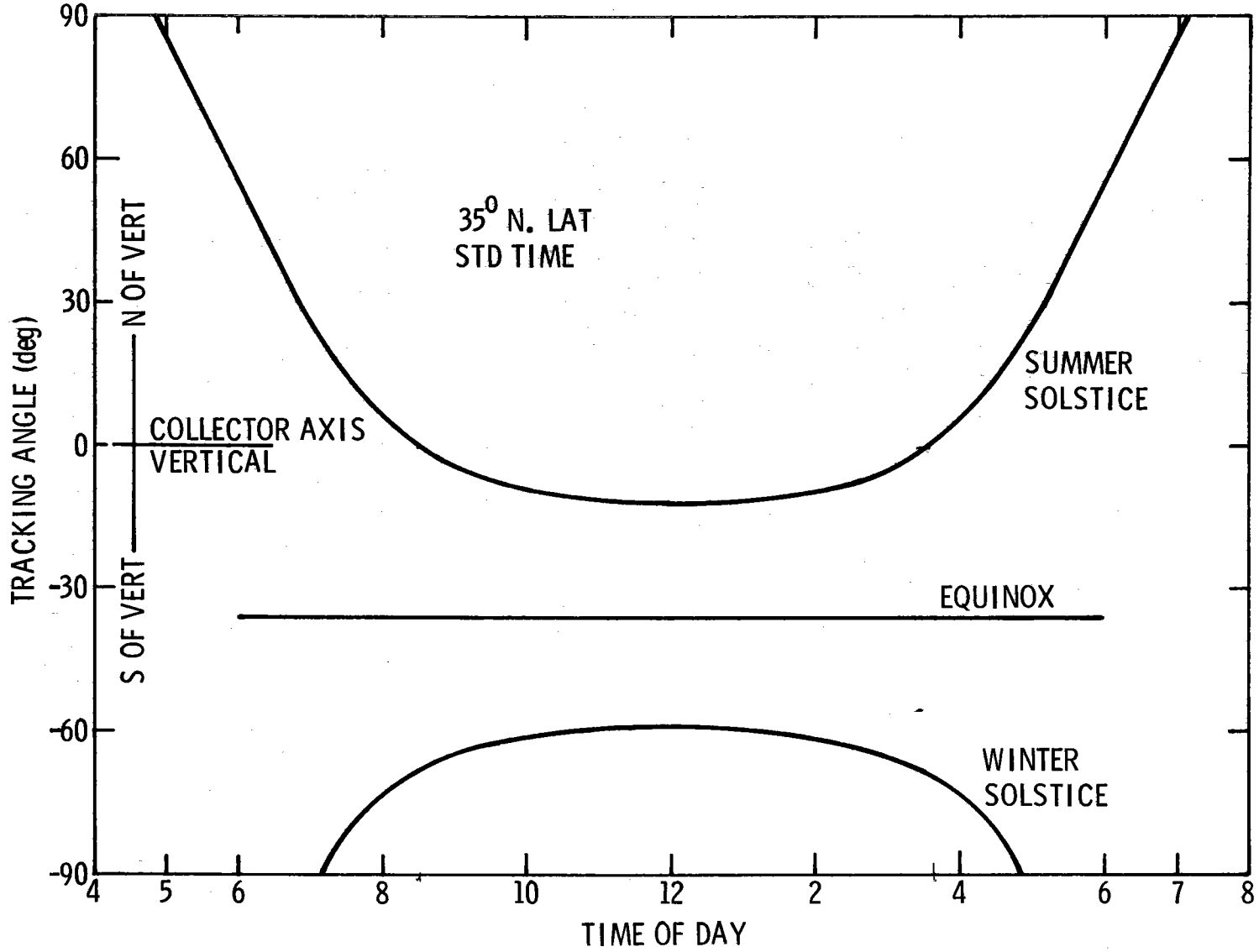

Tracking angle versus time of day for E/W collector

The power usage for a 1/6-HP motor pulsed for 17.5 msec every 12 seconds for 8 hours would be

(10A) (137V) = × 42 seconds = 57,540 watt-seconds.

The pulsed mode uses 57,540 watt-seconds per day per collector or about 0.4 percent of the total power output per day per collector at a turbine efficiency of 13 percent.

Even at 1/6 HP, the motor has been sized very conservatively. In a commercial system, a much smaller motor with a power budget of much less than the 0.4 percent calculated above could be employed.

Tracking System. The tracking system tracking error requirement is less than 0.1 degree and the acquisition angle requirement is 150 degrees or better; therefore, two detectors are used. The coarse detector consists of two silicon photovoltaic cells side by side with a shadow mask over about 80 percent of both cells (Figure 13). If the sun is perpendicular to both cells, the output voltage from both cells will be equal and no error signal results. But, if one cell is illuminated more than the other, an error signal (voltage difference) results. This error signal causes the drive motor to make the needed correction until the sun is within the range of the fine detector.

The fine detector (Figure 14) consists of a cadmium sulfide photopotentiometer located in the center of a 150-mm (6-in.) radius semicircular shaped enclosure. The enclosure is 40 mm (1.5 in.) wide with a 1-mm (0.040-in.) slit running 70 degrees about the center of the 180-degree enclosure. A potential of plus 15 volts is applied to one end of the photopotentiometer and minus 15 volts is applied to the opposite end. If the slit of light falls on the potentiometer precisely in the middle, the resultant output voltage (error signal) is 0. If the slit of light should fall to the right or left of dead center, a plus or minus voltage will result. This error voltage is used to control the drive system to reposition the collector to dead center focus. The interior of the detector is blackened to prevent reflections from causing spurious signals.

System Operation. The coarse detector output (Figure 15) is fed into the differential comparator at the upper left of the schematic. The error voltage from this stage is fed to two operational amplifiers: one an inverter and one a noninverter. The output signal is always positive into R41 because of the diodes CR1 and CR2. If the detector indicates a negative error signal, the inverter stage will invert the signal and pass it through CR2. If the error signal were positive, the noninverter would pass the signal through CR1. The fine detector voltage is handled in much the same way, except without the differential comparator.

On both the inverting operational amplifier for the coarse and fine circuits, a voltage is tapped off at the output of the inverter and fed to a 10-turn potentiometer. These, in turn, are fed to Q8 and Q9, which control a solid-state switch. This solid-state switch controls Q5, which controls the reversing relay K2. If K2 is actuated, the motor on the collector will run in a reverse

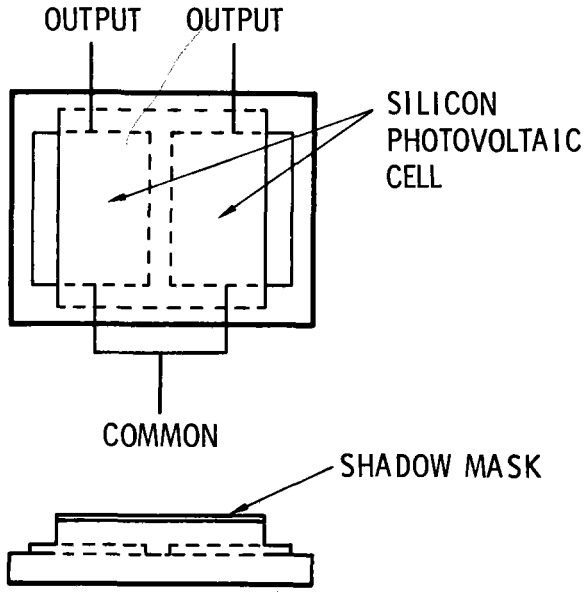

Figure 13. Coarse detector

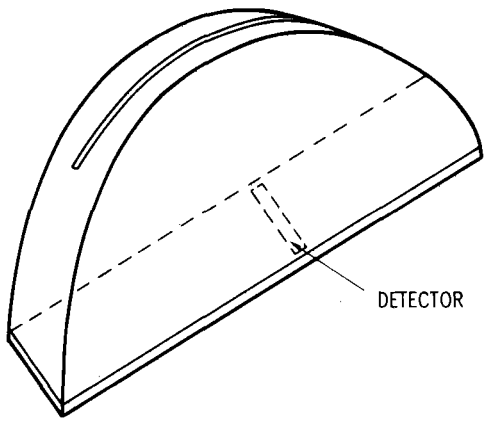

Figure 14. Fine detector

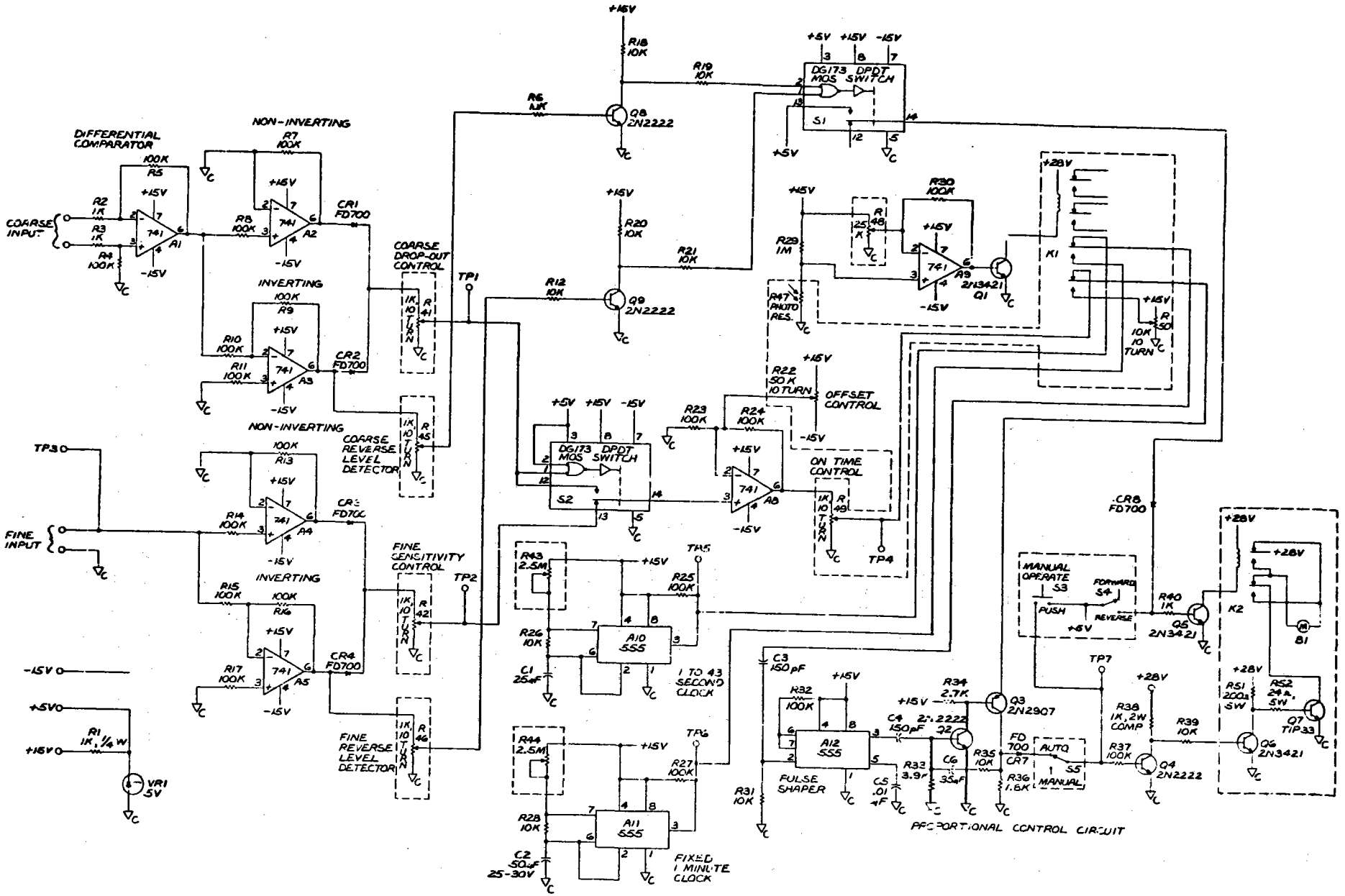

Figure 15. Schematic, solar tracking circuit

direction. If the K2 relay is not activated, the motor will run in a forward direction. The error signal from R41 activates the solid-state switch, which applies the error signal to an operational amplifier with an offset control. The offset control may be used to make any minor adjustments in tracking errors or can be used to set the collector off focus a given amount and still track. The error signal is fed from the R49 to Q3 emitter in the proportional control circuit. Two clocks control the proportional control circuit: a fixed 1-minute clock and a variable 1- to 43-second clock. If the variable clock is set to give a pulse every 12 seconds, that pulse is fed to A12, a pulse shaper which triggers the proportional control circuit. This trigger turns on Q1 and Q3, and both remain on until C6 charges through R35. How long C6 takes to charge up is a function of the magnitude of the error voltage applied on the emitter of Q3. Therefore, with a fixed C6 and fixed R35, the output pulse width across R36 will be a function of the error voltage at the emitter of Q3.

R47 is a photoresistor which detects the intensity of the sun. If the sun's intensity should drop below a given value set by R48, relay K1 is activated by Q1. This causes a fixed voltage to be applied to the emitter of Q3 and the fixed 1-minute clock to be activated. If the sun's intensity stays below a given value for 1 minute, the clock puts out a pulse which activates the proportional control circuit. This fixed clock has no function in the E/W configuration and is deleted for that application. The output pulse then controls Q4, Q6, and Q7, which control the "on" time of the DC motor B1. The motor may also be controlled manually by switches S3, S4, and S5.

Task 3.4 - Fluid Transfer System

Collector Field Layout. The fluid transfer system for the collector field consists of the pipelines, pumps, and control valves for circulating the heat transfer fluid through the field. When the full collector field is in operation, T-66 will be pumped from the cool side of the high-temperature storage tank, through the collectors, and back to the high-temperature side of the tank at a peak heat flow rate of 1.34×10^6 kj/hr (1.27×10^6 Btu/hr).

As described earlier, the 20 collectors to be installed during Phase IV-A will be arranged in two rows, each of which contains 10 collectors, whose axes are colinear and are oriented in an E/W direction. The rows are further divided into sets of five "slaved" collectors whose receiver tubes are joined in a flow-through configuration. The center-to-center spacing between rows is 7.6 m (25 ft). The question of the optimum number of rows and columns in a collector field array has been the subject of considerable analysis. For any set of constant operating conditions, the receiver performance improves as the fluid flow rate increases, primarily because of increased heat transfer associated with the greater turbulence. This implies that a large number of collectors in series, each of which contributes a small temperature gain, is desirable. However, these gains are limited eventually by the fact that the required pumping power increases with flow rate. Therefore, a maximum number of collectors may be effectively used in series.

Figures 16 and 17 show efficiency and ΔT versus flow rate (1) for a single collector, 3.66 m in length and (2) for three sizes of flow restrictor plugs. Dramatic increases can be observed up to a point where the curves tend to flatten out.

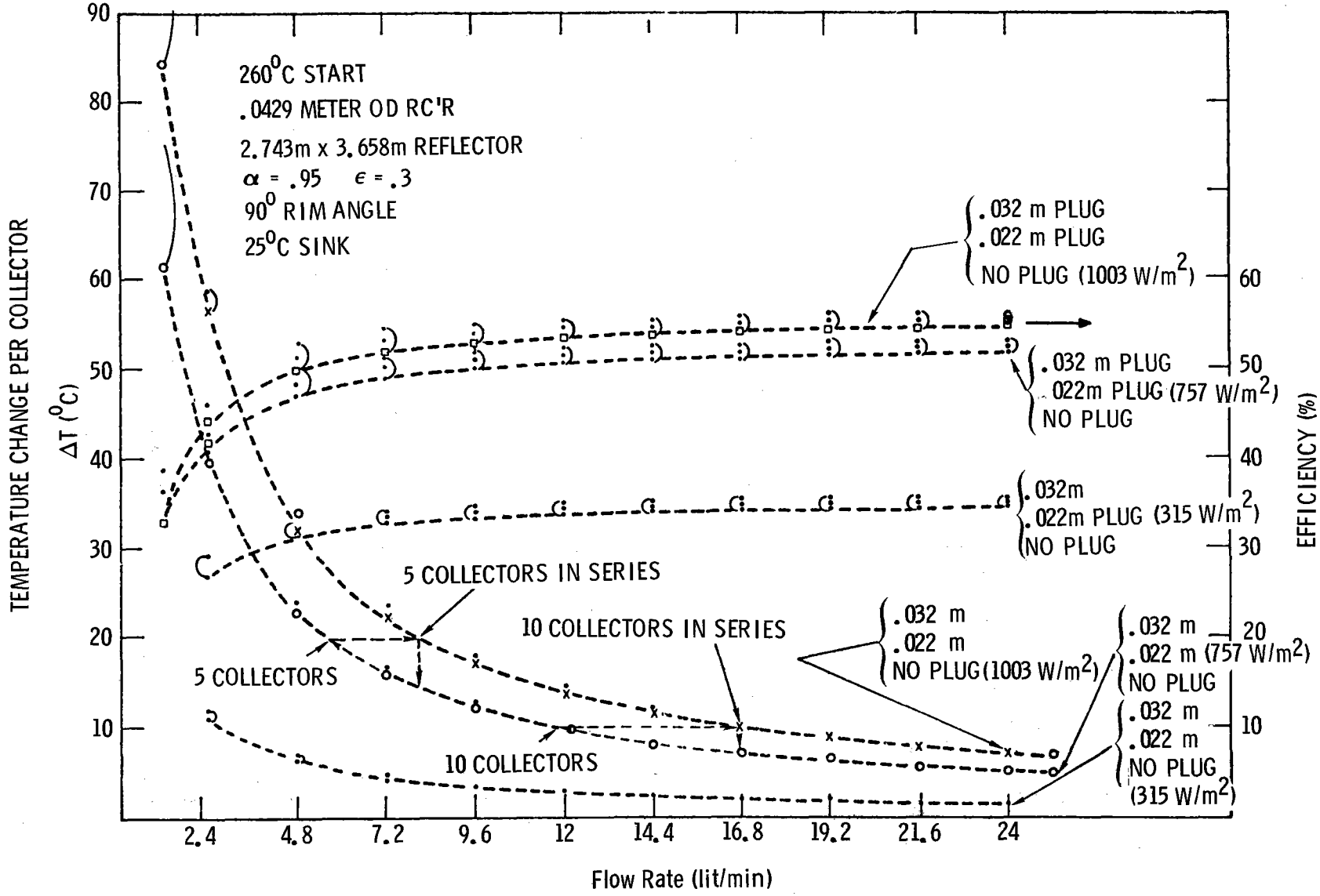

Figure 16. Flow rate versus efficiency versus collector ΔT

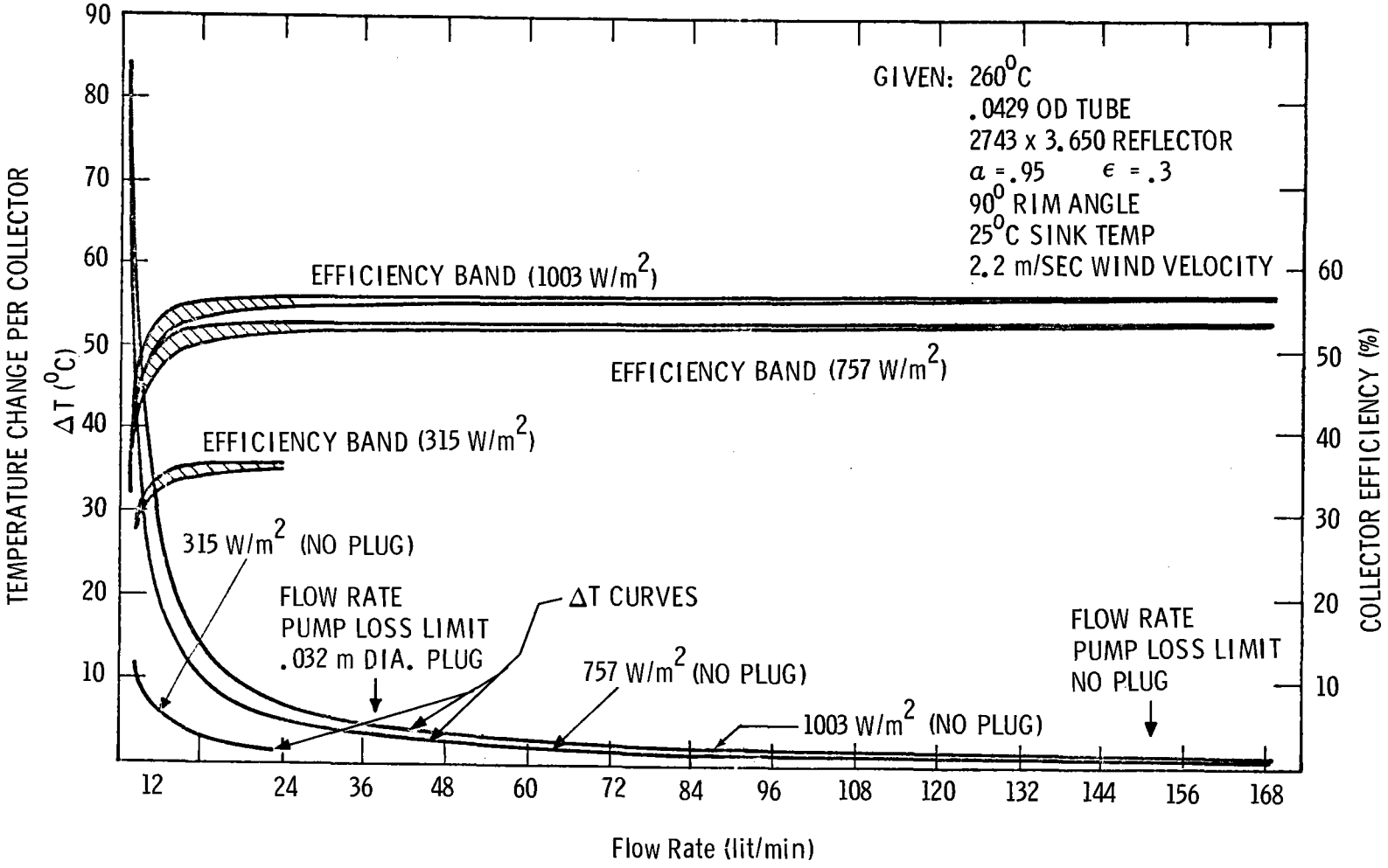

Figure 17. Collector efficiency and ΔT versus flowrate

For instance, at a normal solar insolation of 1000 W/m^2, a flow rate of 7.9 lit/min results in a temperature rise of 20°C per collector. Should the insolation decrease to 750 W/m^2, the flow rate must be reduced to 5.4 lit/min to maintain the same temperature rise per collector. The efficiencies corresponding to those flow rates approach the knees of the respective efficiency curves; if the insolation drops lower (as a result of water vapor, cirrus clouds, etc.), the flows must be reduced to a point where laminar fluid flow in the receiver tubes results in low efficiencies. However, if more collectors are placed in series, the temperature increase per collector is less. Consider halving the ΔT in the above example to a 10°C ΔT per collector (which implies doubling the number of collectors in series); the required flow at 1000 W/m^2 is 17 lit/min; at 750 W/m^2, it is 11.5 lit/min; and, at 315 W/m^2, it is 2.8 lit/min. For most of this flow range, the collectors operate on the efficiency plateaus, and the energy collected remains relatively high.

The underlying assumptions, not stated in the figure, are that the input temperature to the array is 210°C and the required output is 310°C for a ΔT through the array of 100°C. Therefore, linear behavior from the 260°C conditions shown on the figure is assumed. This is not an unreasonable assumption.

The high side of the allowable flow-rate range can be determined by calculating, for a given array and attendant pipeline configuration, that flow rate at which pumping losses begin to exceed receiver efficiency gains. In the case of an E/W collector field, the calculation is complicated by the fact that insolation varies continuously over a wide range because of incidence angle effects (Figure 18). As a result, many plumbing arrangements must be modeled individually, and their performance must be integrated over a daylong period by computer techniques. The integrated performance of a number of plumbing arrangements is listed in Table IV.

The collected pump energy per day referred to in the table is defined as follows. Collected Pump Energy per Day = $\frac{PE}{\eta_p \eta_c}$, where

PE = theoretical pump energy per day, MJ

η_p = pump efficiency = 0.5

η_c = turbine/generator cycle efficiency

= 0.174 (winter)

= 0.154 (summer)

The table indicates that the optimum collector array is 20 in series with 28-mm (1.125-inch) diameter plugs; this will be considered the baseline array.

For greater flexibility in engineering tests, the pipelines and valves will be arranged so that the collector field can be operated as four parallel rows of five, two parallel rows of ten, or a single row of 20 collectors. Figure 19 is a schematic layout of the pipeline design. Any compromise necessary to achieve this flexibility will, however, penalize the 4 x 5 and the 2 x 10 configurations rather than 20 in series. The system will be operated in the off-optimum configurations to verify analyses, to investigate the control problems of series/parallel operation, and to obtain general engineering data.

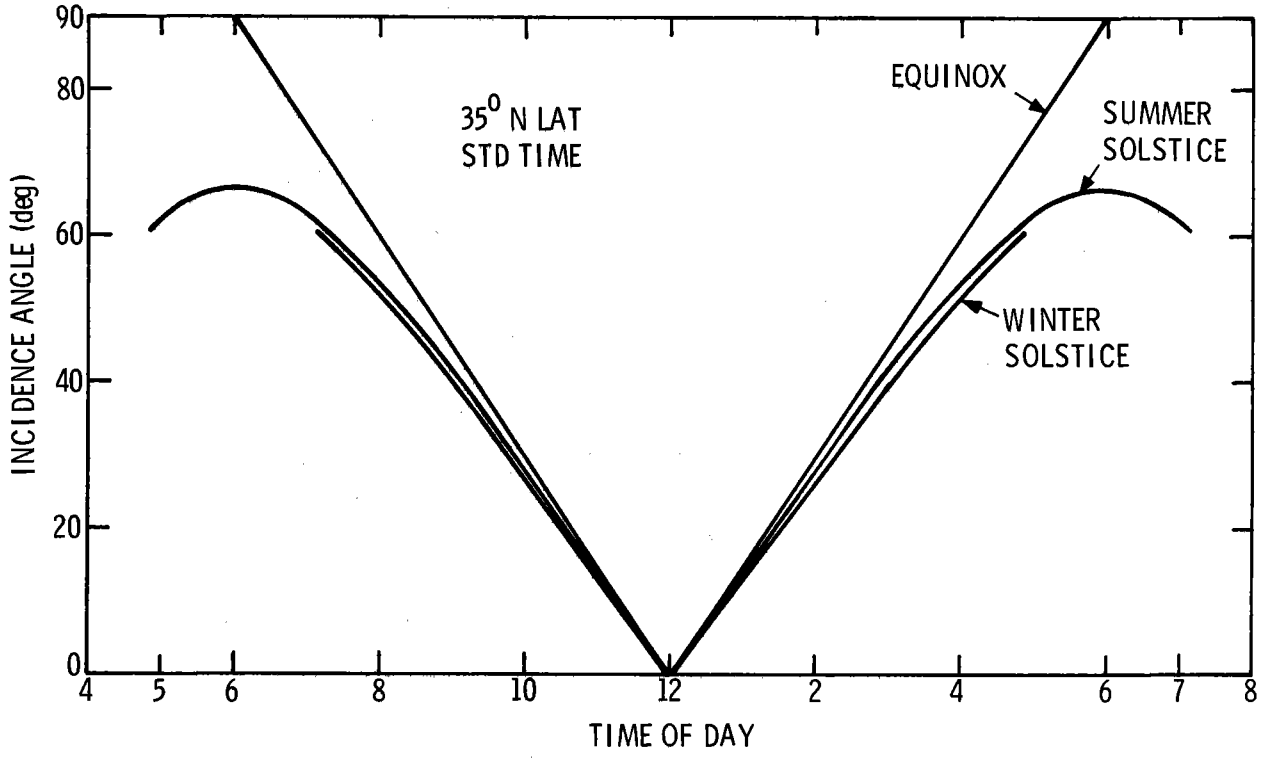

Figure 18. Solar incidence angle (cosine effect) versus time of day for tracking E/W collector

TABLE IV

Integrated Collector Performance

Plumbing Arrangement	Summer Solstice Net Energy (MJ)	Winter Solstice Net Energy (MJ)
10 in series, no plugs	2616	2244
10 in series, 28-mm plugs	2731	2301
10 in series, 32-mm plugs	2751	2320
20 in series no plugs	2762	2323
20 in series, 25-mm plugs	2794	2351
20 in series, 28-mm plugs	2796	2352
20 in series, 32-mm plugs	2775	2333

Net energy = total collected energy per day
- collector field thermal loss per day
- collected pump energy per day

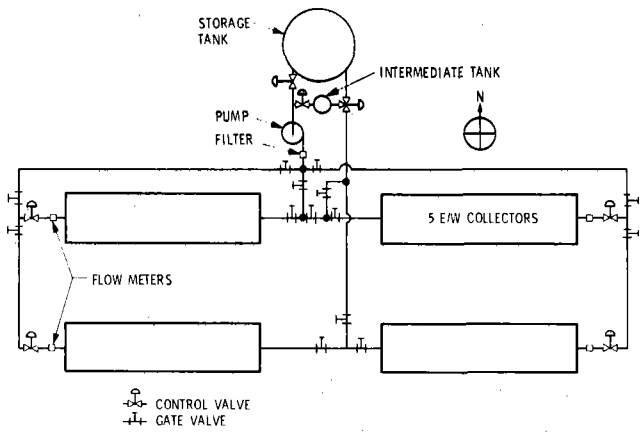

Figure 19. Schematic layout of pipeline design

Pipeline Design. The pipeline will consist of thin-walled steel tubing (1.65-mm wall). The advantages of tubing over steel pipe for this system are (1) that tubing is available in thinner walls than pipe and for a given diameter will be less expensive than pipe, (2) the low thermal mass of the tubing reduces heat losses during morning warmup, (3) small hydraulic fittings may be used with tubing as opposed to the large flanges necessary with steel pipes, (4) the small fittings will have a smaller thermal mass and can be insulated better, and (5) tubing can be bent to form the necessary elbows and expansion joints resulting in less head loss.

The insulation chosen for the pipeline consists of a layer of ceramic fiber blanket next to the tubing and a layer of rigid polyurethane foam on top of the blanket. This combination was chosen on the basis of cost comparison with several other options of equal performance. A sketch showing the details of construction is shown in Figure 20. Insulation thickness was sized by balancing the value of the energy being saved versus the cost of the insulation. An energy value of $5/GJ (4.75/MBtu) and an insulation cost amortization rate of 10 percent were assumed. On this basis, an insulation thickness of 50 mm has been chosen for the case of the 1.0-inch tubing. Figure 21 shows how the optimum insulation thickness varies as a function of assumed energy value.

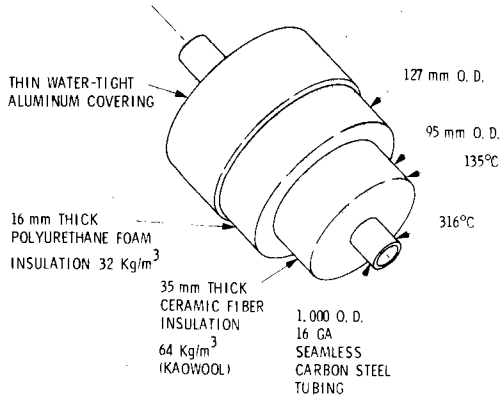

Figure 20. Construction of insulated pipeline

The tubing diameter was sized at 1.0 inch by analyzing the total collector field losses per day for various tubing diameters. The results are shown in Figure 22. In this figure the total loss per day equals insulation thermal loss per day plus collected pump energy per day minus the frictional heat generated per day. The frictional heat is that generated by the fluid friction in the pipeline and components.

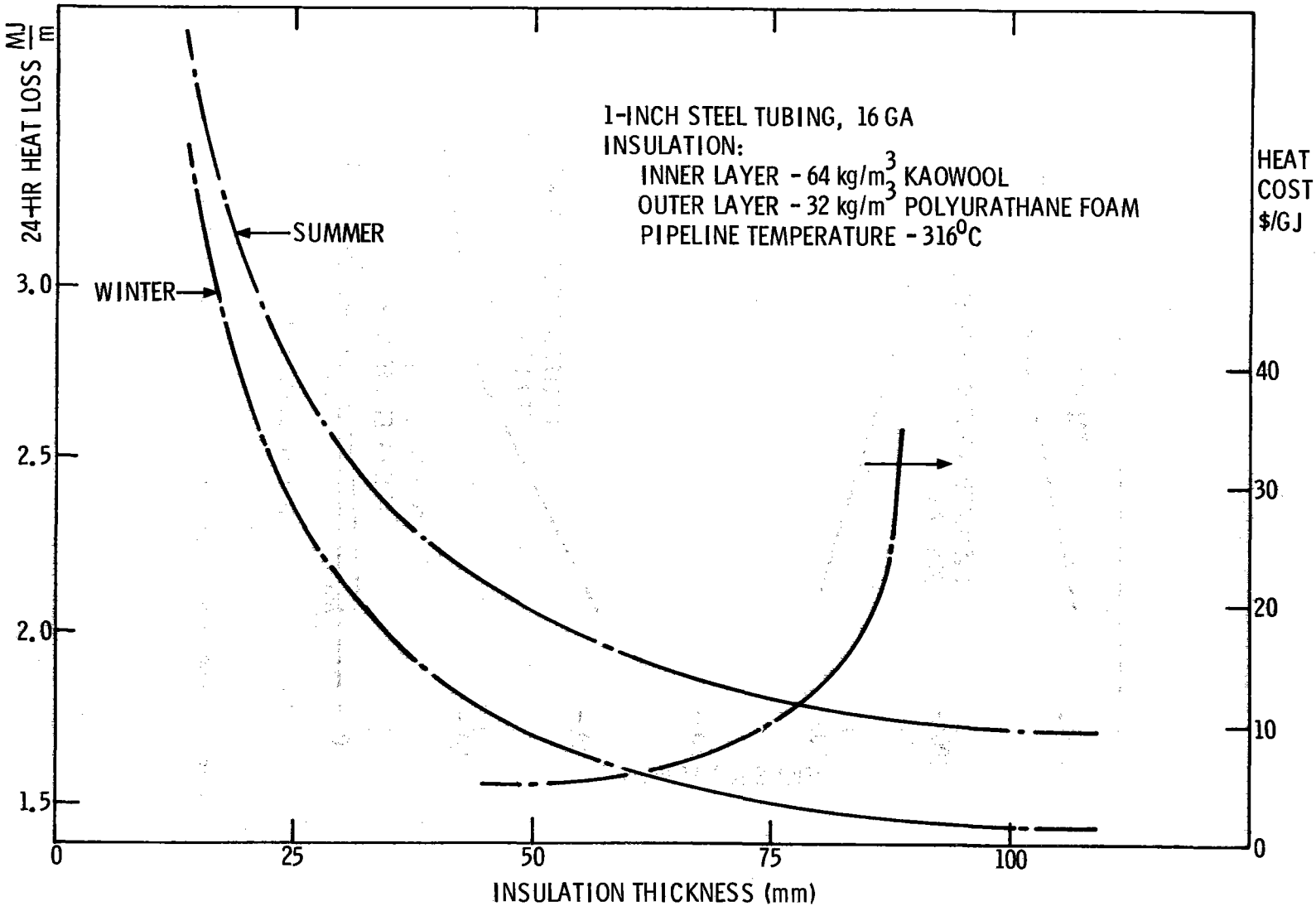

Figure 21. One-inch steel tubing, 16 gage

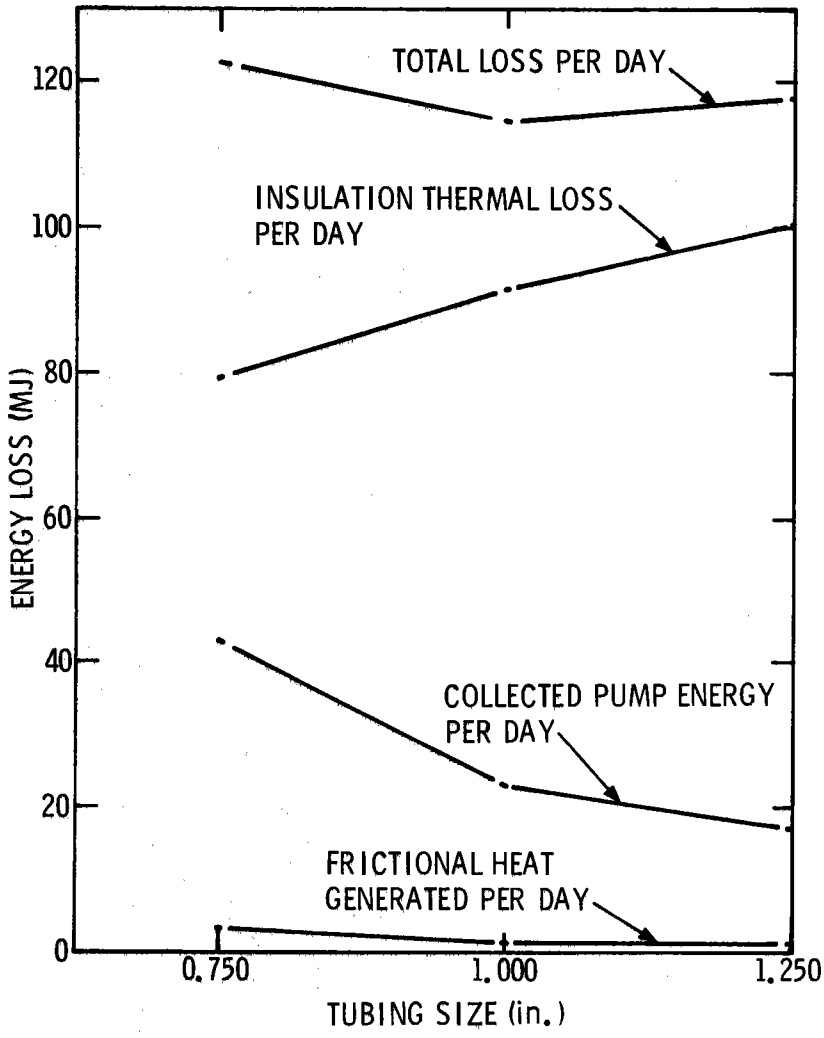

Figure 22. Energy losses per day versus tubing size for summer solstice

Task 3.5 - Cooler

As a consequence of the change in the baseline design, the requirements for this component have changed. The cooler must now be capable of dumping heat at rates in excess of the collector field output of 1.34×10^6 kJ/hr (1.27×10^6 Btu/hr) and the turbine/generator demand of 0.77×10^6 kJ/hr simultaneously. The cooler will also be used to decrease the temperature of the stored T-66 from 311°C to 48°C (590-118°F) at a rate of 1.2×10^6 kJ/hr.

Requests for performance of an air-cooled heat exchanger adequate to meet the requirements are presently being solicited from equipment manufacturers. In that air-cooled heat exchangers do not normally afford tight control on the fluid outlet temperature, the cooler selected will be capable of undercooling the fluid, and a constant fluid return temperature will be maintained by bypassing the hot fluid around the exchanger and blending it with the return fluid.

Task 4 - High-Temperature Storage

A storage evaluation facility is being designed and fabricated by Sandia Laboratories, Livermore, to evaluate storage problems, particularly those pertinent to the thermocline concept. The 7570-liter (2000-gal) facility has been designed for use with low-vapor-pressure heat transfer fluid up to 316°C (600°F) or with pressurized water up to 232°C (450°F) and 3100 kPa (450 psi). The facility is schematically shown in Figure 23. The system has oil heaters to simulate the collector input at heating rates up to 348,000 kJ/hr (330,000 Btu/hr). It also has water-cooled heat exchangers capable of transferring 167,000 kJ/hr (160,000 Btu/hr) to represent the output to the turbine.

Upon the conclusion of testing by Sandia at Livermore, the systems will be partially dismantled and shipped to Albuquerque for inclusion in the Solar Total Energy Project as the high-temperature storage component. At present, all of the piece parts for the facility have been received except for the main tank whose delivery is anticipated in October. The tank and heat exchangers must be pressure tested before final assembly. It is estimated that the system will be ready for delivery to Albuquerque in late spring or early summer of 1975.

Task 5.1 - Boiler

The heat exchanger to transfer the heat from the T-66 fluid to the turbine fluid (toluene) has been selected and a purchase order initiated. The heat exchanger will consist of three series-connected Heliflow exchangers manufactured by Graham Manufacturing Company. These exchangers are counterflow types which offer the advantages of efficient operation and small size. Small exchangers are easier to insulate against heat losses.

The exchangers were designed to operate the system turbogenerator at 40 kW, with a 232°C (450°F) boiling temperature and 304°C (580°F) superheat temperature. At 40-kW conditions, a 10°C (18°F) pinch point is predicted between the Therminol 66 and the toluene. The heat exchanger, which is approximately 0.9 meter (3 ft) in diameter by 2.4 meters (8 ft) long, has a total heat transfer area of 26.1 m^2 (281 ft^2). If the system is operated at 32 kW and at 246°C (475°F) boiling temperature, the pinch point should drop to around 5.5°C (10°F). The pinch point, which is the closest temperature approach of the T-66 fluid to the toluene fluid along the length of the heat exchanger, determines the temperature drop attainable in the T-66 heating fluid passing through the exchanger. A 0-degree pinch point would represent the maximum heating fluid temperature drop but would require a heat exchanger of exceptionally large area.

Task 5.2 - Turbine

In the selection of an energy conversion cycle, it is generally desirable to achieve as high an efficiency as possible. If one looks at the most ideal cycle on a temperature-entropy (T-S) plot it has the shape of a rectangle (Figure 24). Such an ideal cycle is never attainable because one is constrained to follow the state point lines of the particular working fluid in question.

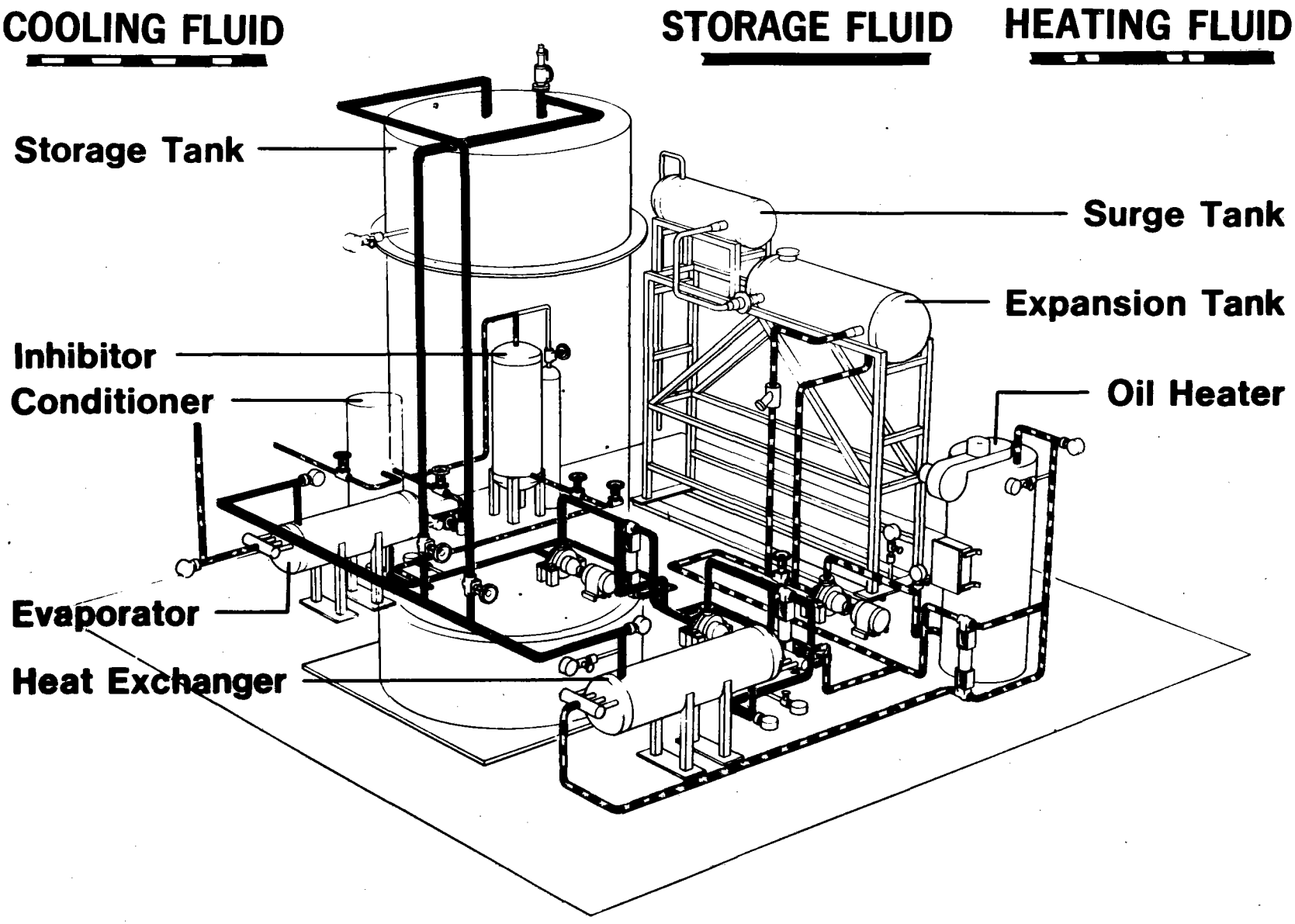

Figure 23. Prototype Solar Energy Storage Bank

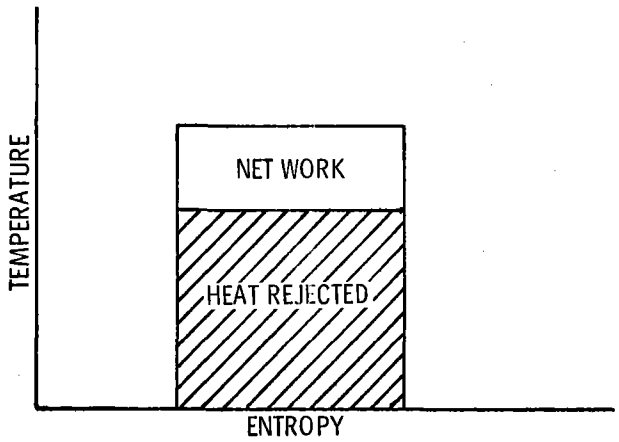

Figure 24. Temperature-entropy plot-ideal cycle

The most common working fluid is water; its T-S plot is represented in Figure 25. The thermodynamic cycle 1, 2, 3, 4, 5 represents simplified standard practice for a steam system. A major constraint on a steam system is the avoidance of liquid water in the turbine during expansion, i.e., the expansion process from 1 to 2 cannot cross the saturated vapor line at point 2. To avoid this, the vapor must be superheated, 5 to 1, as shown.

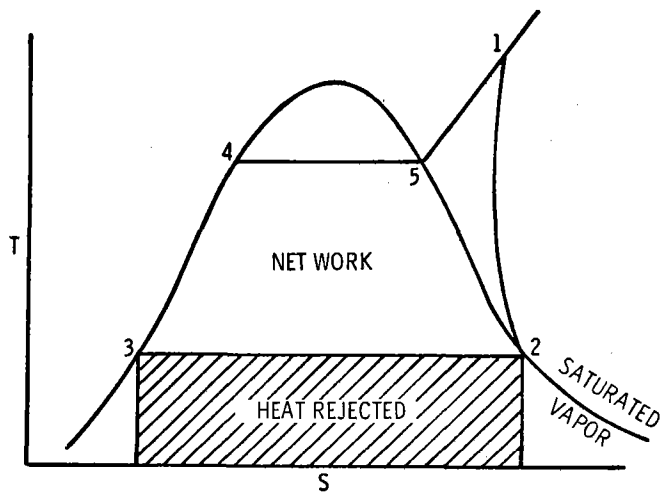

Figure 25. Temperature-entropy plot H_2O

The T-S diagrams of another general class of fluids (includes high-molecular-weight organics) are represented in Figure 26. Notice that the saturated vapor line has a positive slope and that expansions from it end in the superheated region; thus, the problem of liquid droplets in the turbine is avoided. This is why an organic working fluid was chosen for the solar thermal energy conversion system. A further bonus of the high-molecular-weight organic is its low nozzle spouting velocity which allows the turbine to run at lower speed and to accomplish the entire expansion in a single stage. All of these characteristics reduce system cost.

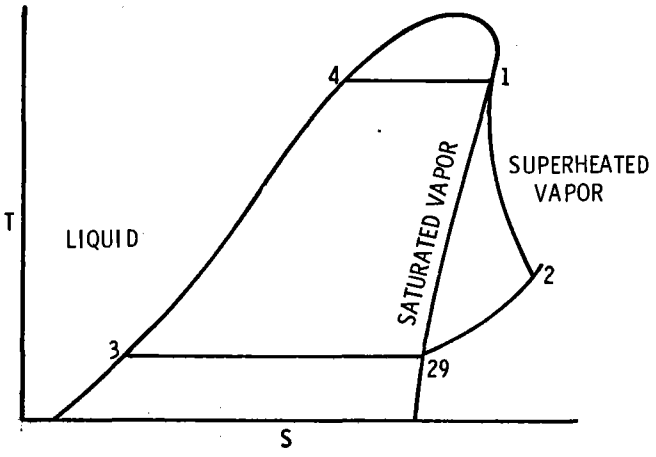

Figure 26. Temperature-entropy plot typical organic working fluid

Sundstrand Aviation has been involved for several years with the development of small turbine/generator systems. One developed in conjunction with the American Gas Association is a 100-kW gas-fired total energy system that uses toluene as a working fluid in a supercritical cycle. This Sundstrand system is being modified to operate at the inlet, outlet, and output conditions required in the Solar Total Energy System. The purchase order for these modifications was placed in late September. Delivery of the completed system is scheduled for May 15, 1975. The specified operating conditions are 304°C (580°F) superheated toluene at the turbine inlet and 93°C (200°F) to 48°C (120°F) condenser temperatures. Electrical output capability is 32 kW.

Task 5.3 - Rankine Loop Heater

The turbine/generator set being procured for the program was originally designed as a gas total energy package; therefore, it contains a gas-fired heater. The piping on the turbogenerator set will be rerouted so that this heater can serve as the storage and Rankine loop heater. The heater is capable of providing approximately 3.16×10^6 kJ/hr (3×10^6 Btu/hr) to the T-66 loop. The heater will be available upon receipt of the turbine/generator in May 1975.

Task 5.4 - Turbine Heat Exchanger

The turbine load heat exchanger constitutes the interface between the condenser cooling loop and the cooling tower loop. This exchanger is to keep the cooling tower water, which becomes contaminated by the evaporation process, out of the condenser and low-temperature storage. A "Graham Heli-Flow" counterflow heat exchanger will be used. Capable of transferring 632,000 kJ/hr (600,000 Btu/hr), it is available for installation.

Task 5.5 - Cooling Tower

The air conditioner and turbine cooling tower, an induction-type cooler supplied by Baltimore Air Coil Inc., is capable of dissipating 2.1×10^6 kJ/hr (2×10^6 Btu/hr) with 36°C (96°F) ambient and 21°C (70°F) wet-bulb temperature. This tower utilizes the induction spray cooling concept and consequently does not require fans with their attendant noise. The basic cooling tower, cooling-tower pumps, and piping to run from the remote tower to the turbine building are presently available.

Task 5.6 - Load Bank

The load bank for the generator is a stepped resistor type with a capacity of 49 kW, 3-phase, balanced-load, 60-Hz, 480 volts with forced-air cooling. The steps are as follows:

Step Number	1	2	3	4	5	6	7	8	9	10	11
Capacity (kW)	10	10	5	5	5	5	5	1	1	1	1
Total (kW)	10	20	25	30	35	40	45	46	47	48	49

Any combination of these steps may be used. The load bank, which is currently available, has provisions for remote operation from the motor control center and a thermal cutoff in the event of overheating.

Task 6 - Instrumentation and Control System

Turbine and Control Building. A 140-m^2 building will be constructed to house system components and control equipment. This building (Figure 27) will house all major system equipment except collector field, high- and low-temperature storage, and cooling tower. Detailed design of this building is 85 percent complete; and it is estimated it will go to bid in November. Site, location, and exterior appearance are presented in Figure 2.

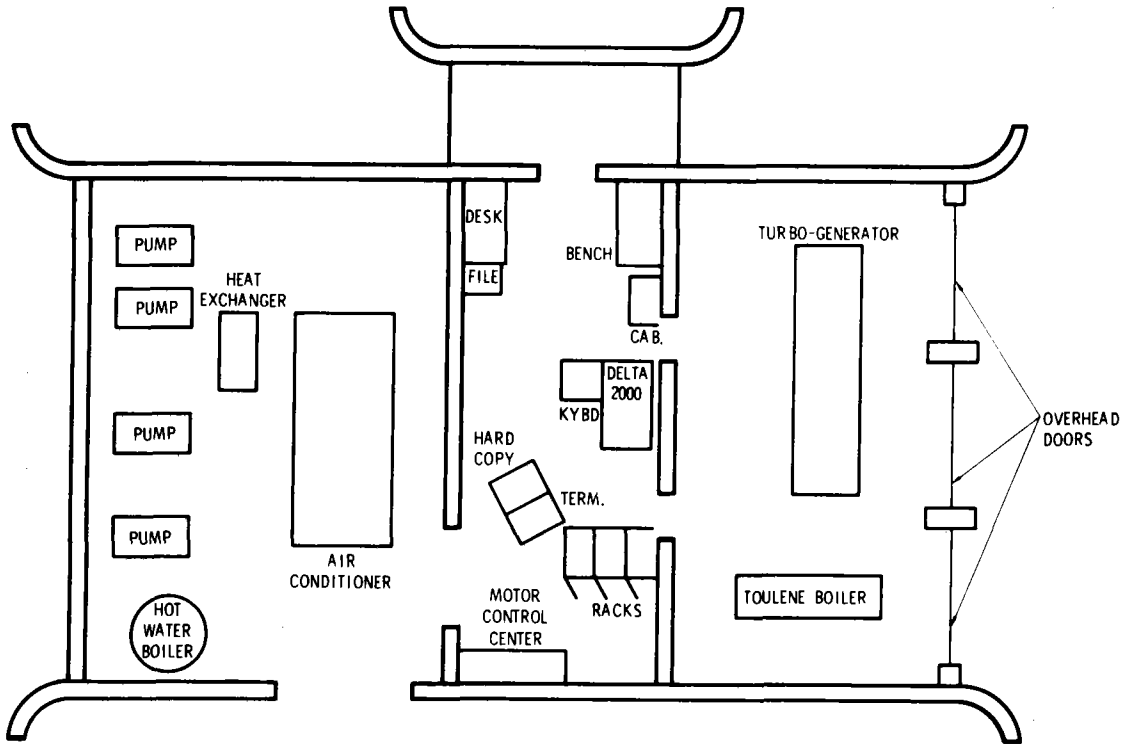

Turbine and control building floor plan

Instrumentation. Approximately 75 percent of the instrumentation and control equipment described in the last quarterly report has been delivered. Major items still required are (1) interface electronics between Hewlett-Packard minicomputer and Honeywell Delta^{R} control-monitor equipment, (2) minicomputer expended memory, (3) system valve and pump controllers, and (4) system sensors.

Computer Program CONTRL. The purpose of the collector field control system is to maintain a constant, preset working fluid temperature in the high-temperature storage tank during system start-up, shutdown, insolation fluctuations, and steady-state operation. To determine suitable control strategies which can maintain this temperature restriction, a computer program, CONTRL, which analytically models the transient heat transfer of the parabolic solar collector field, was written. The model includes the transient heat transfer in the distribution pipes and the collectors and calculates the fluid temperatures along the field for given flow rates, ambient conditions, and solar insolations. The intent of all control strategies will be to determine the required system operating parameters for maintaining a set working fluid temperature into the high-temperature storage.

Control Systems and Strategies. Several preliminary start-up control strategies have been examined and implemented with the analytical model during this reporting period. Initial outputs of the analytical model showed that, because of the very high transient heat loss of the pipes at start-up, field output temperatures at start-up cannot be maintained at the set point. Several control system arrangements will be tested to determine what to do with this low-heat-quality output fluid. Some of these arrangements are (1) recirculating the low-quality fluid and letting it supply the entire fluid input to the field, (2) holding the low-heat-quality fluid in an intermediate tank and blending it into the field input line with the low-temperature storage fluid, or (3) blending continuously the recirculated fluid into the main line with low-temperature storage fluid by using a small blending tank in series with the main fluid input line (blending is used to inhibit abrupt changes in temperature into the input line).

The control system tested during this reporting period is Arrangement 2. Control for this arrangement is shown in Figure 28.

The heat exchange fluid leaves the bottom of the storage tank at a temperature of 218°C. From point A, the fluid travels straight through valve V1 to the pump. The pump may be running at a preset start-up speed or at a speed computed from solar intensity and incidence angle cosine.

At B, the fluid divides to the two collector loops. At Valve V2, the fluid is returned to one pipe to return to the storage area. At Valve V3, the fluid (if its temperature is below 311°C or above) will be diverted to the intermediate tank.

Controller T1 will blend fluid from the storage tank and the intermediate tank to keep input temperatures to the field within a few degrees of the temperature of the storage tank bottom.

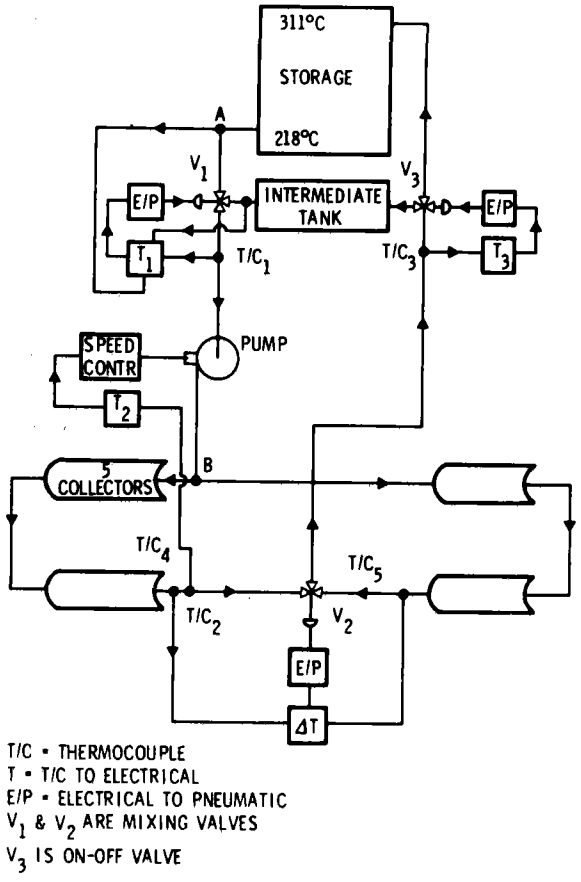

Figure 28. Control system-Arrangement 2

When the temperature at T/C2 approaches the correct operating temperature, Controller T2 starts regulating the pump speed.

Controller ΔT uses input T/C4 as its set-point temperature and, by regulating mixing Valve V2, matches the set-point temperature T/C5; thus, both collector loops will be operating at the same temperature.

The strategy tested with this arrangement is described by the flow diagram in Figure 29. This strategy uses proportional control based on the output temperature. The merit of the strategy is determined by observing (1) the percent overshoot, in temperature of the response (PO); (2) the time, T_s, required to initiate dumping into high-temperature storage; (3) capacity, V_{it}, required for the intermediate tank; and (4) V_s, the volume of fluid dumped into high-temperature storage after 30 minutes.

The time response of this strategy is plotted in Figure 30 along with a table of merit figures. The solar insolation used for these responses corresponds to start-up at 8:00 AM in June. For early-morning start-up, this strategy appears to be suitable. However, early-morning start-up

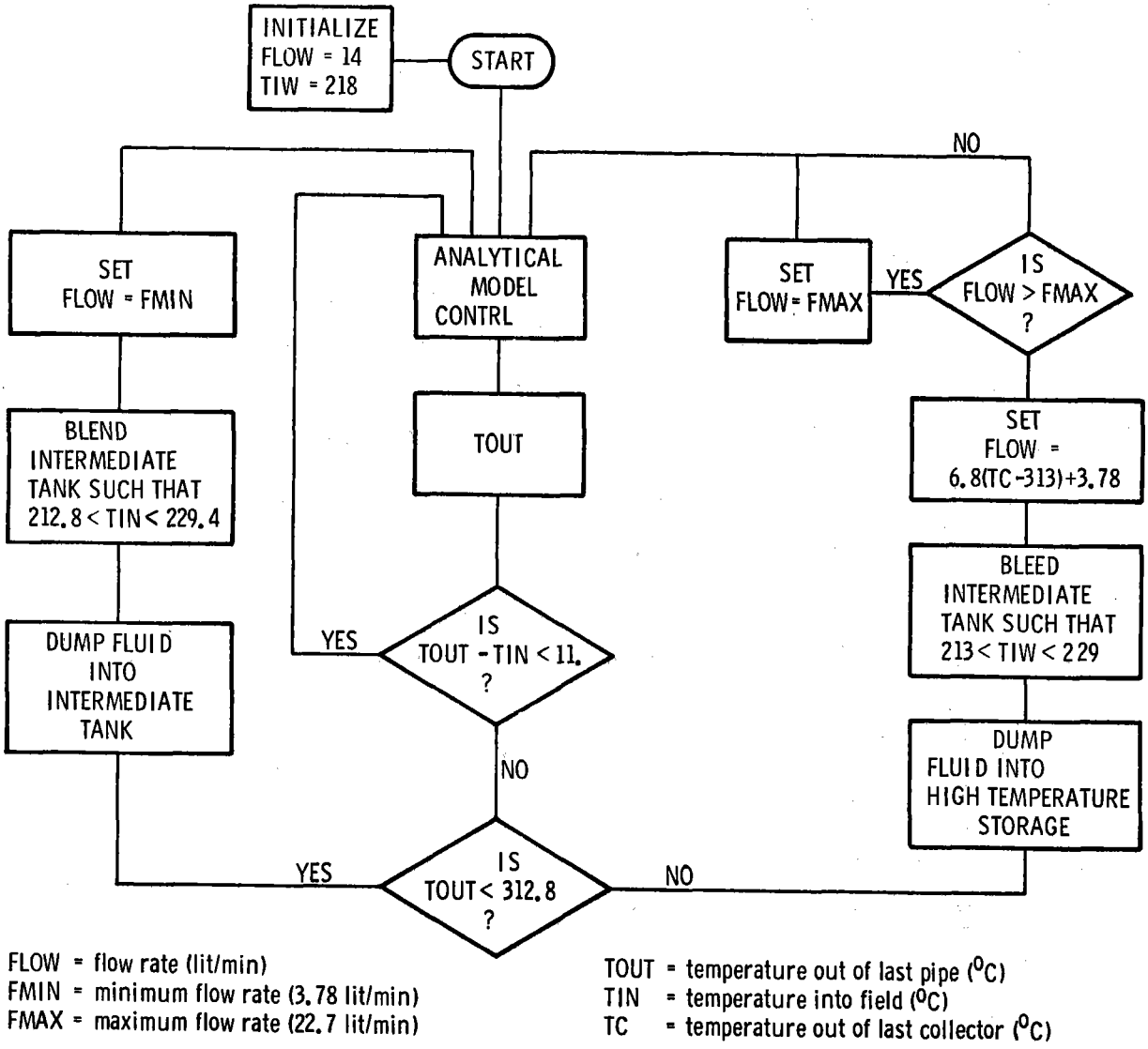

Figure 29. Control strategy flow diagram

is not the same as midmorning start-up because of the different level of solar insolation. Midmorning start-up can occur as a consequence of intermittent clouds. Further studies will include examining control method; different strategies (such as proportional plus derivative control) will be used in these studies, and other solar conditions, such as intermittent clouds, will be considered. It is intended that, once several strategies and arrangements have proven satisfactory, real recorded solar data will be used for isolation to provide a test under more realistic conditions.

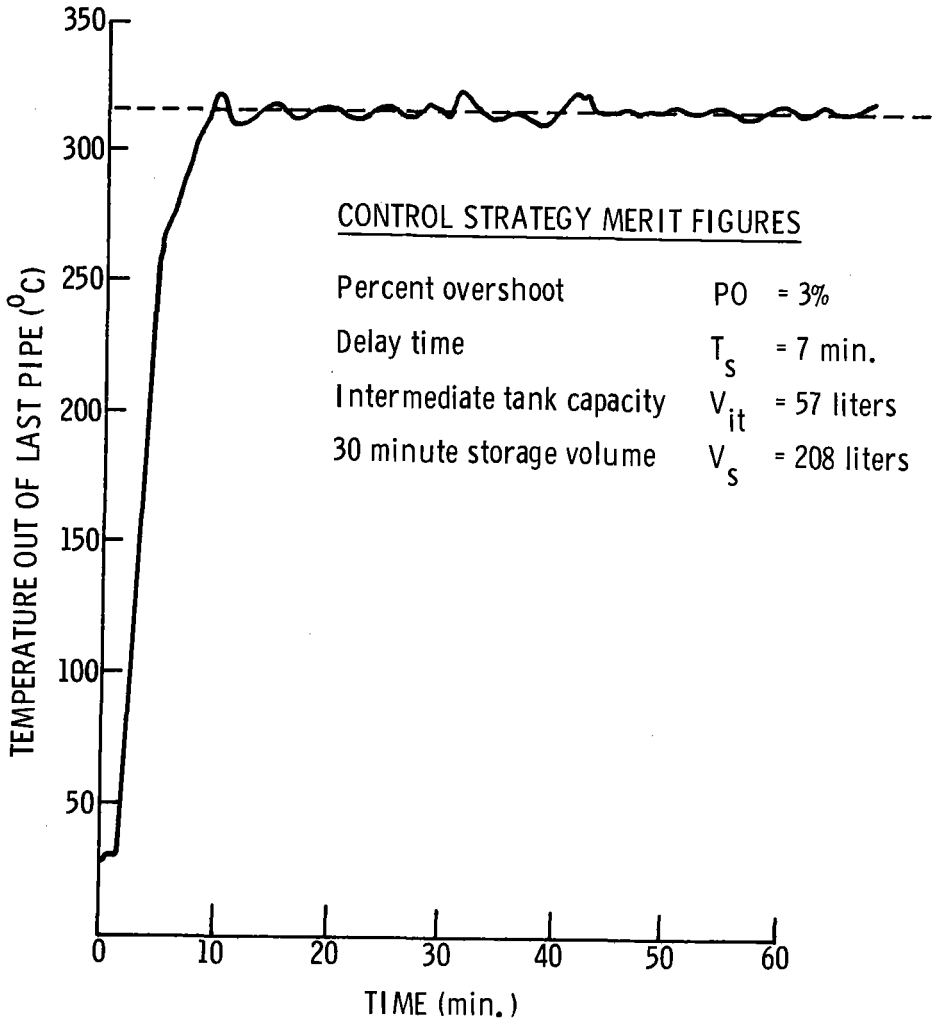

Figure 30. Time response of collector field

Task 7 - Collector Test Facility

Focused Collector Tests. The testing accomplished to date has been primarily for the purpose of validating the quality and accuracy of the instrumentation. As a result of these tests, a more accurate analog-to-digital converter has been integrated into the system, a random thermocouple temperature interrogation and averaging technique has been instituted, and an incremental temperature-measuring technique has been adopted.

Tests for design discrimination will be conducted with a receiver-tube nonselective coating which has an absorptance and total hemispherical emittance slightly less than 1.0. Temperature changes resulting from design changes are greater and can therefore be more accurately measured when the emittance is high.

Test comparisons of various vacuum levels in the receiver-tube glass envelope are now in progress; these tests will progress to the comparison of receiver-tube plugs which force annular flow.

In Figures 31 and 32, some recent test data are compared with analytically predicted results. The relatively close agreement suggests a high degree of reliability in the analytical model of the system.

North-South Installation. A two-unit N/S focused collector installation is being made at Sandia's Collector Test Facility; the two 2.74- x 3.66-m (9- x 12-ft) units were fabricated by the MFG Boat Company. These two units will be mounted with each rotational axis aligned N/S and the north end tilted up to 45 degrees. The welded steel pipe support frameworks are spaced 4.87 m (16 ft) center to center in an east-west direction. Concrete pads will be provided for the four corners of the framework along with suitable tie-down facilities to withstand the 1364-kg (3000-lb) maximum loads (both up and down) caused by high wind loads on the 10-m^2 area of the trough.

This two-unit installation should provide the capability for thorough evaluation of most of the parameters of a multiunit north-south focused collector field, and comparison with extensive system analyses now being done.

The framework and drive mechanism were designed and procured by Sandia's TTR Development Division.

Flat Plate Tests. A preliminary test was run on a flat plate collector. The scatter in test results was excessive and as a result some rework of the collector and the data acquisition computer program is being accomplished.

Glass that has been treated to reduce reflection will be incorporated for the next test. The reduced reflection treatment was developed by Sandia's Ceramics Development Division. Transmissivity of the glass has been improved by about 4 percent with this treatment.

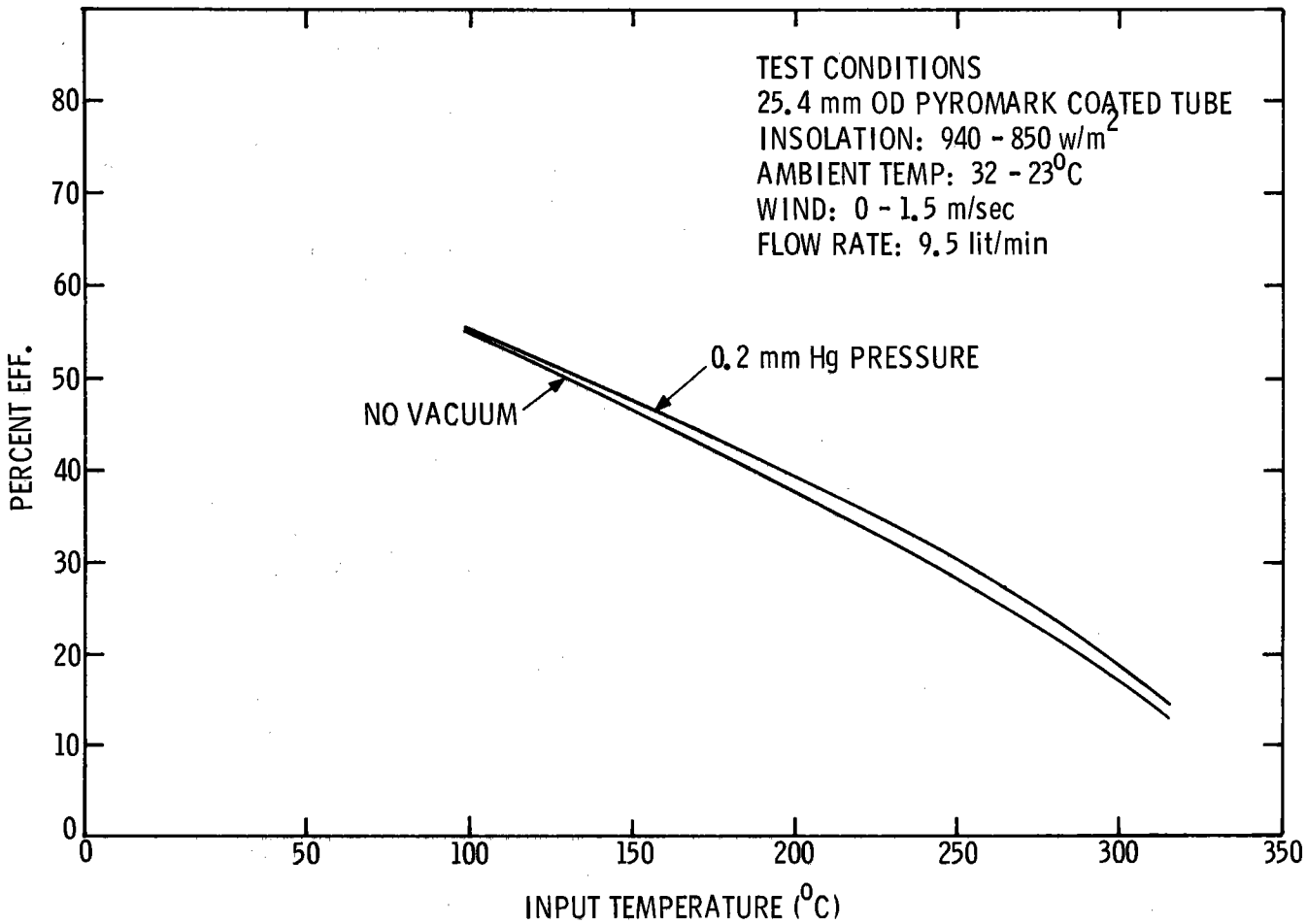

Figure 31. Parabolic trough collector test results

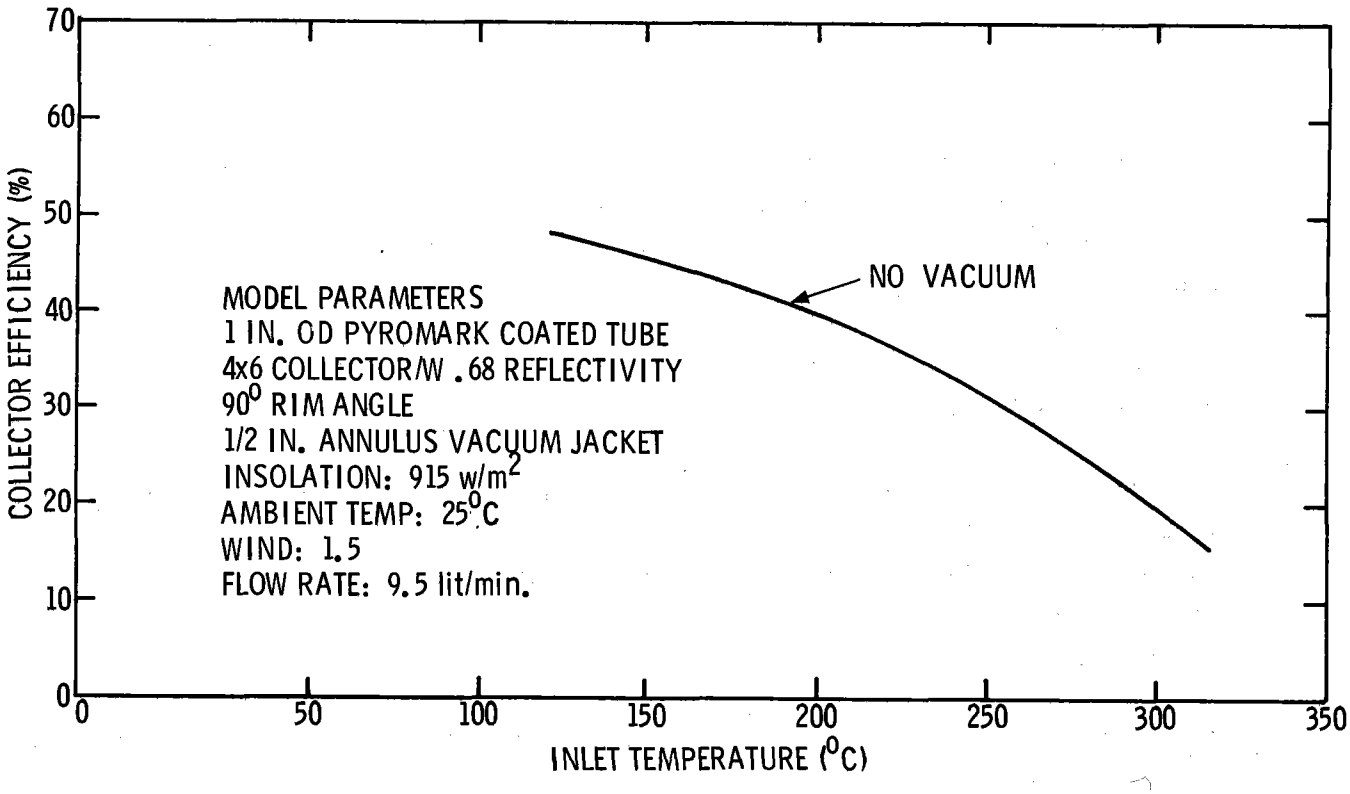

Figure 32. Parabolic trough analytic results

Task 8.1 - System Load Profiles

A computer program providing building heating and cooling loads has been completed. However, the program is capable of simulating only a single load zone (e.g., a house). This program, called HLOAD, which has been integrated into the Solar Energy Systems Simulation Program (SOLSYS), is providing calculated load data based upon heat loss through the walls, floor, and ceiling; incident solar energy; infiltration; and thermal mass of the Solar Project Building.

To provide the flexibility needed to accurately model the mixed loads of other solar energy systems, such as a solar community, the Computer Program for Analysis of Energy Utilization in Postal Facilities (commonly referred to as the P. O. Program) has been obtained from General American Research Division of General American Transportation Corporation. This program has the capability of successfully modeling a multizoned building such as low-rise apartments which might be found in a typical new community.

The original version of the P. O. Program has been modified for ease of use with SOLSYS. In that the solar community concept at Sandia is not at the stage where detailed building design parameters are known, it was decided to provide SOLSYS with a building-loads information routine which would allow easy modification of gross structural features (such as number of apartments in a complex) so that load data for various types of buildings could be quickly generated. Towards this end, the P. O. Program was modified to compute loads for buildings having rectangular shapes only. The modified program is called BLDGN.

The restriction of rectangular shapes allows tremendous simplification of the input data required by the P. O. Program. A low-rise apartment is simulated by assuming that, given a defined unit (normally a single apartment), the apartment complex may be generated through repetition of this unit. Thus, to simulate a two-story apartment complex one apartment deep and three wide, the single apartment characteristics are defined, and the complex is then defined as one apartment deep, three apartments wide, and two stories high. Fenestration is handled by defining the percent of each outside wall which constitutes window. BLDGN internally places one window of this size in the center of each vertical outside wall.

An additional modification in BLDGN is the inclusion of a thermal mass to allow temperature drift between maximum and minimum thermostat settings. This is felt to more realistically model actual conditions than maintenance of a constant inside temperature as in the P. O. Program.

The results of a preliminary BLDGN load computation are shown in Figure 33, where the effect of grouping load zones (in this case apartments) on the per unit load can be seen. The two-story apartment complex represented by Curve b is comprised of six apartments identical to that represented by Curve a. Each apartment is 72 m^2 (850 ft^2); air conditioning is supplied to keep the apartment temperature below 22°C (72°F). Also, each outside vertical wall is defined as 10 percent glass for windows. The loads are presented on a unit basis to demonstrate the tendency of one apartment to insulate another; thus the energy demands are lowered.

(a) Single Apartment - 79 m^2 (850 ft^2)

(b) One-sixth of load for two story complex with three apartments (79 m^2) each story.

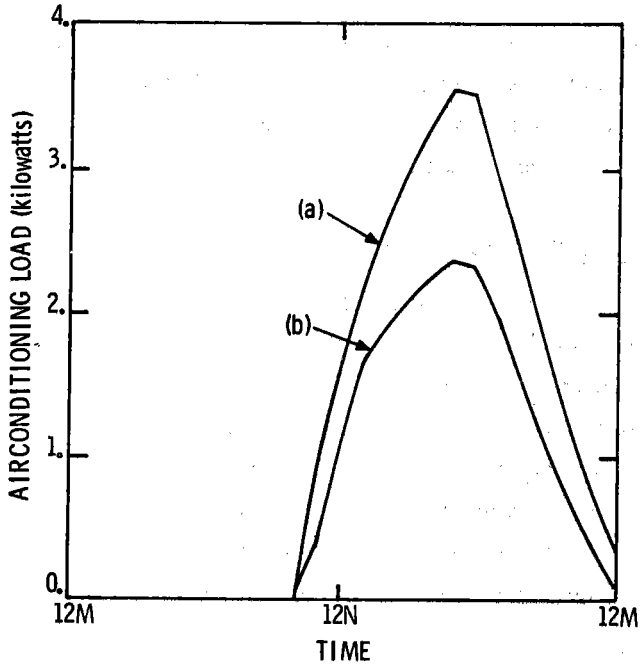

Figure 33. BLDGN load computational results

Future modifications are planned to allow BLDGN to combine rectangular shapes so that buildings other than rectangular in overall shape may be simulated, i.e., L-shaped buildings.

The Public Service Company of New Mexico has furnished electric power consumption data for a 474-home middle-class subdivision in Albuquerque, NM. This information provides electric power demand at 15-minute increments spanning a 15-month time interval from May 1973 through July 1974. The reduced data provide an average electric power load history per customer within the subdivision.

In addition to the residential data, further load history data representative of the commercial and industrial segments of the electric power consumers group has recently been received. Among the facilities for which data were supplied are the following:

- A large city high school.
- A large city hospital and extended medical care facility.
- A large combined grocery-discount merchandise shopping facility.
- A large Sears Roebuck store.

- An FAA airways control center.
- A local manufacturing plant which produces wallboard.

These data in general span the 1973 calendar year.

The data will be compiled to provide a catalog of facilities for which electrical load histories are available as input to the SOLSYS program. This will provide the program user with the option of selecting various mixes of residential-commercial-industrial electric power consumers to incorporate in solar total energy studies.

Task 8.2 - Solar and Weather Input Data

Because insolation varies with time of day and year, geographic location, and climate, the information needed for realistic analyses is very complex. Moreover, the solar energy collection schemes under consideration demand a subdivision of insolation into types. Solar-cell development involves knowledge of the different wavelengths of solar insolation. Flat-plate solar collectors are capable of absorbing total solar insolation, which includes diffuse radiation from the solar disc. Concentrating collector development requires data on the direct beam insolation, because concentrators cannot focus diffuse radiation. These data are especially important because virtually all schemes designed for the conversion of solar to electrical energy use collectors requiring direct beam insolation.

A number of records of total insolation measurements exist; about 80 U.S. weather stations maintain records. However, only daily totals and monthly averages of the total insolation for these weather stations have been regularly published. To get more frequent readings, tapes must be obtained from the U.S. Weather Bureau. Moreover, the records on total insolation are known to contain uncertainties caused by numerous factors such as different calibration procedures, different instrument types, and instrument deterioration. These uncertainties have been estimated to be as high as 20 percent. The appropriate corrections for each instrument are not yet known.

Information on direct beam insolation is extremely limited. Only four stations in this country have records of direct insolation measurements: Blue Hill, Massachusetts; Omaha, Nebraska; Albuquerque, New Mexico; and Tucson, Arizona. Thus, no data on direct insolation exist for most geographic and climatic loactions in this country.

Several different techniques for estimating solar insolation have been published. Some of these are based primarily on theoretical derivations, others are purely empirical, and still others use a combination theory and data analysis. Most are procedures for estimating total insolation or direct insolation under clear-sky conditions; virtually no detailed work has been done on the frequency and duration of dimming or occultation of the solar disc by clouds.

In an effort to improve this situation, Sandia Laboratories has begun an attempt to significantly improve the status of insolation information, particularly information regarding direct insolation. Two specific goals have been formulated. The first of these is to devise a method for estimating direct insolation based upon date, time, geographic and climatic location, total insolation, and common weather parameters such as visibility, cloud cover, and precipitable water-vapor content. This would permit the creation of direct insolation "records" from past weather records at any location where these data are available. The formula will be derived from a number of sources: existing formulas, the large body of real data for Albuquerque, and statistical analyses. The formula will be tested with another set of real data for Albuquerque. It is expected that a formula considerably more accurate than any which now exist can be derived.

The second goal is to derive statistical distributions of those weather parameters which significantly affect insolation, such as cloud cover, cloud patterns, atmospheric water-vapor content, and visibility, for several locations in the U. S. These frequency distributions, along with the formula for direct insolation, would make it possible to simulate solar insolation conditions. The distributions will be derived empirically from existing records. An attempt will be made to take into account not only cloud frequency and duration but also cloud location. This factor is extremely important because, for example, opaque clouds covering the entire western half of the sky have little influence on focusing collectors in the morning, while these same clouds reduce direct insolation to zero after noon. Very little analysis of cloud location has been done before.

Currently, Sandia is working principally on the first goal mentioned. A fairly comprehensive search for past results and similar efforts has been made. Published estimation techniques are now being compared with real data from Albuquerque. Albuquerque insolation and weather data are being statistically analyzed to determine which weather parameters influence solar insolation.

Concurrently, a large body of data is being readied for analysis and comparison. Specifically, two weather tapes containing hourly solar intensity and weather data for the years 1962 and 1963 have been obtained from the National Climatic Center: (1) WBAN Hourly Surface Observations 144 Tape and (2) Solar Radiation Hourly 280 Data Tape. These tapes contain weather and solar information on an hourly basis for the following eight cities: Albuquerque, Boston, Fort Worth, Los Angeles, Miami, Asheville, Omaha, and Seattle. These eight cities were chosen because the tapes were available and because the cities represent a good cross-section of the various types of weather conditions found in the United States. For example, Boston has a high heating requirement in the winter combined with low solar intensity. On the other hand, Miami has low heating but high cooling requirements combined with high-solar intensity. It is felt that these cities constitute a wide enough spectrum of heating, cooling, and solar loads to determine where and under what constraints the solar total energy concept is viable.

The Solar Radiation Hourly 280 Data Tape has been decoded. Decoding of the Hourly Surface Observations 144 Tape is in progress and should be complete early in the next quarter.

Because the Climatic Center tapes do not contain continuous solar data, Sandia has also obtained copies of all the total and direct insolation strip-chart recordings made at the Albuquerque Weather Station for every day of 1962 and 1963. These are being read at 10-minute intervals to provide extensive solar insolation data for this period.

Task 8.3 - Alternate Total Energy Systems

The SOLSYS system analysis program is being used to perform studies of several model solar total energy communities. The first of these alternative community designs being analyzed is composed of 1000 individual homes separated by 35 m (120 ft). Each home has 140 m^2 (1500 sq. ft) of floor space and the electric, heating and cooling, and hot water demands are supplied by the total energy system. The location is Albuquerque, N. Mex. Figure 34 is a schematic of the system as modeled by the computer program.

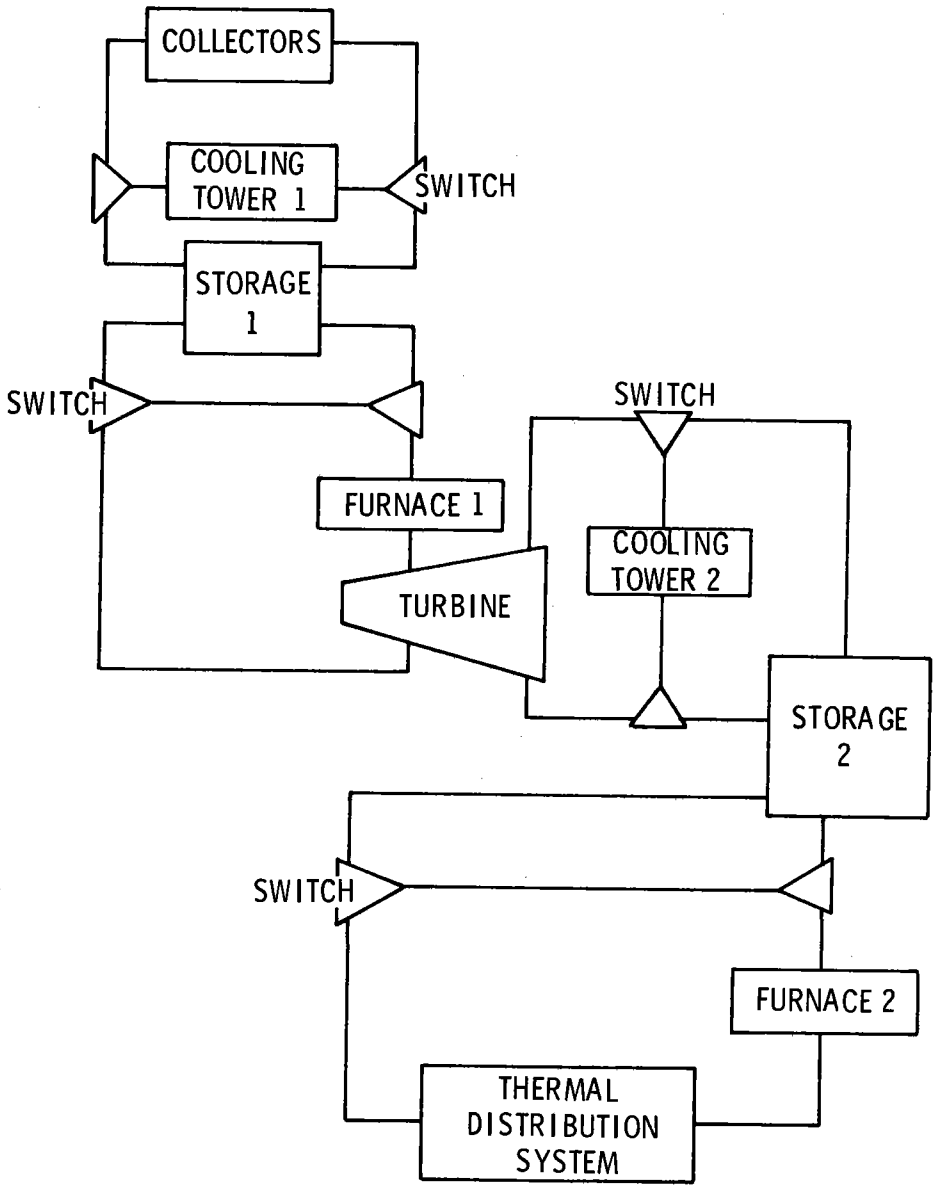

Figure 34. Schematic for Solar Community Total Energy System

The primary components are an array of focusing parabolic collectors, high- and low-temperature storage systems, a turbine/generator for electrical generation, two cooling towers to dissipate energy when the storage systems are full, two fossil-fuel auxiliary furnaces to provide supplementary energy, and a thermal distribution system to distribute thermal energy to the homes. Clear-air solar intensities for Albuquerque were utilized as solar input, and the thermal loads were computed with the HLOAD subroutine. Computations are made every half-hour for four 4-day periods (solstices and equinoxes). These 16 days were then used to represent a year. A problem inherent in this assumption is that it does not take into account the month or more thermal lag of the earth, i.e., maximum and minimum temperatures do not occur on solstices, and days requiring no heating or cooling do not coincide with the equinoxes. As more detailed solar and weather data become available (see Section 8.2), they will be incorporated in the SOLSYS program to eliminate this problem.

The thermal and electrical loads on the system and the house temperature response are independent of the portion of energy supplied by the solar energy system and thus can be discussed separately. Figure 35 is a plot of the ambient air temperature and the resulting house temperature for the four reasons. The house temperature is permitted to vary between 20°C (68°F) and 25°C (77°F). This relatively tight control on the house temperature requires the system to heat and cool during the equinoxes. In practice, a greater temperature variation is allowed during the spring and fall. Consequently, during the spring and fall, the temperature at night is permitted to drift downward below the lower limit. Also, during spring, the infiltration rate is sharply increased during the daytime hours; this simulates window opening, when the solar load on the house tends to drive the house temperature above the upper temperature limit. The ragged response in the house temperature curve around noon in the spring period is a result of this increased infiltration.

The loads on the homes for each of the periods are shown in Figure 36. The electric loads, which vary throughout the day, average near 1.0 kW per house. The mean hot water demand is approximately 0.6 kW, with a peak near 0.9 kW. Cooling is required during summer and fall, and heating is required during winter and spring. These curves contrast the seasonal variation in thermal demands with the relatively constant electric and hot water demands. During summer and fall, the thermal requirements are 230 and 190 MJ/day, respectively, and those for heating in spring and winter are 200 and 590 MJ/day. Clearly, the thermal demands are significantly higher for winter than for other seasons. Further, other choices of spring and fall days may reduce those thermal requirements significantly and make the difference greater.

To provide energy for this community, N/S single-axis tracking collectors elevated to 35 degrees were chosen. Each collector was 9.14 m wide by 15.15 m long, and the total number of collectors was varied. The collectors heated Therminol 66 to 317°C (602°F) for use in the boiler of a Rankine-cycle system which used toluene as the working fluid. The toluene was superheated to 307°C (584°F) with boiling and condenser temperatures of 211°C (411°F) and 94°C (200°F),

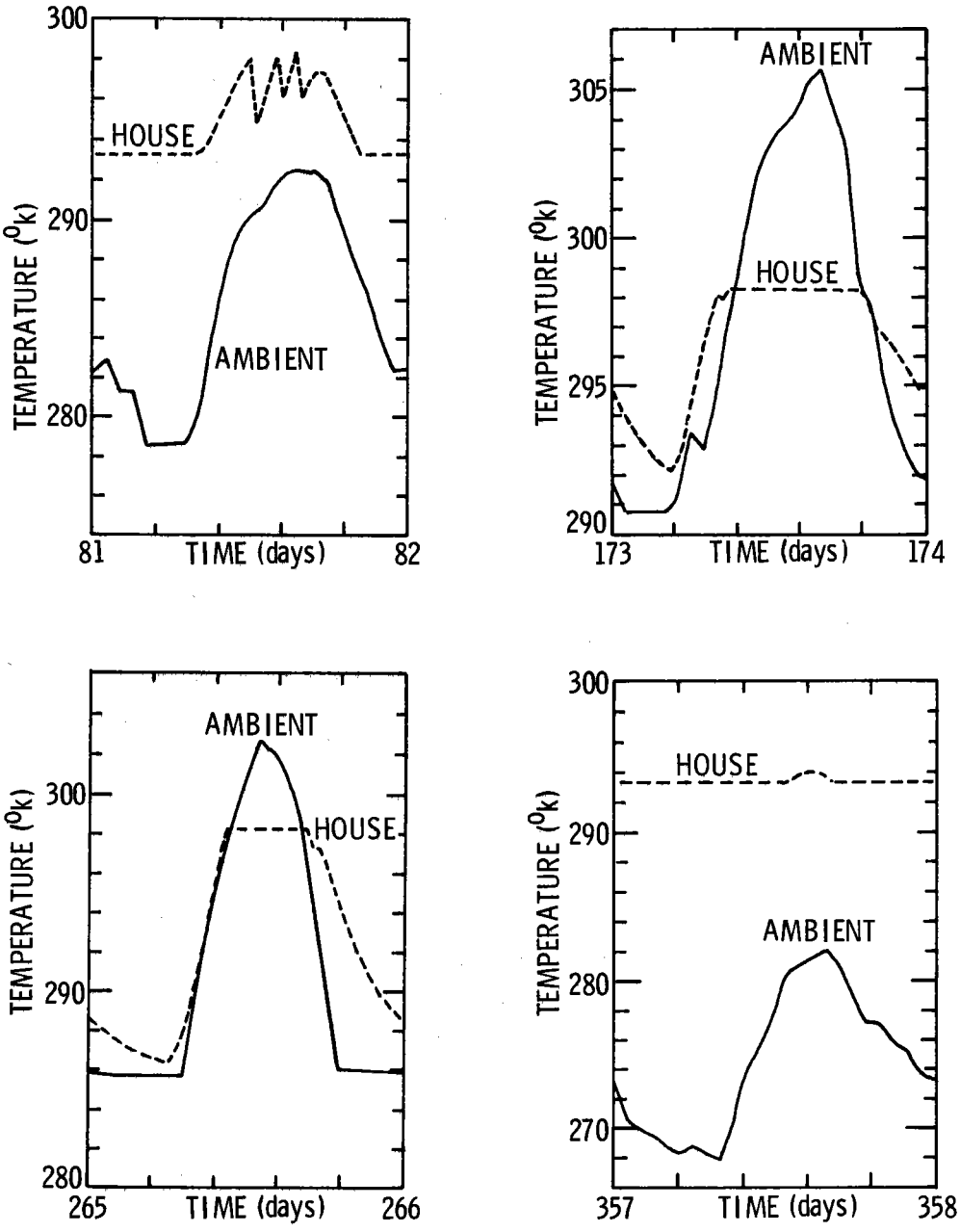

Figure 35. Ambient air temperature and house temperature (Albuquerque location)

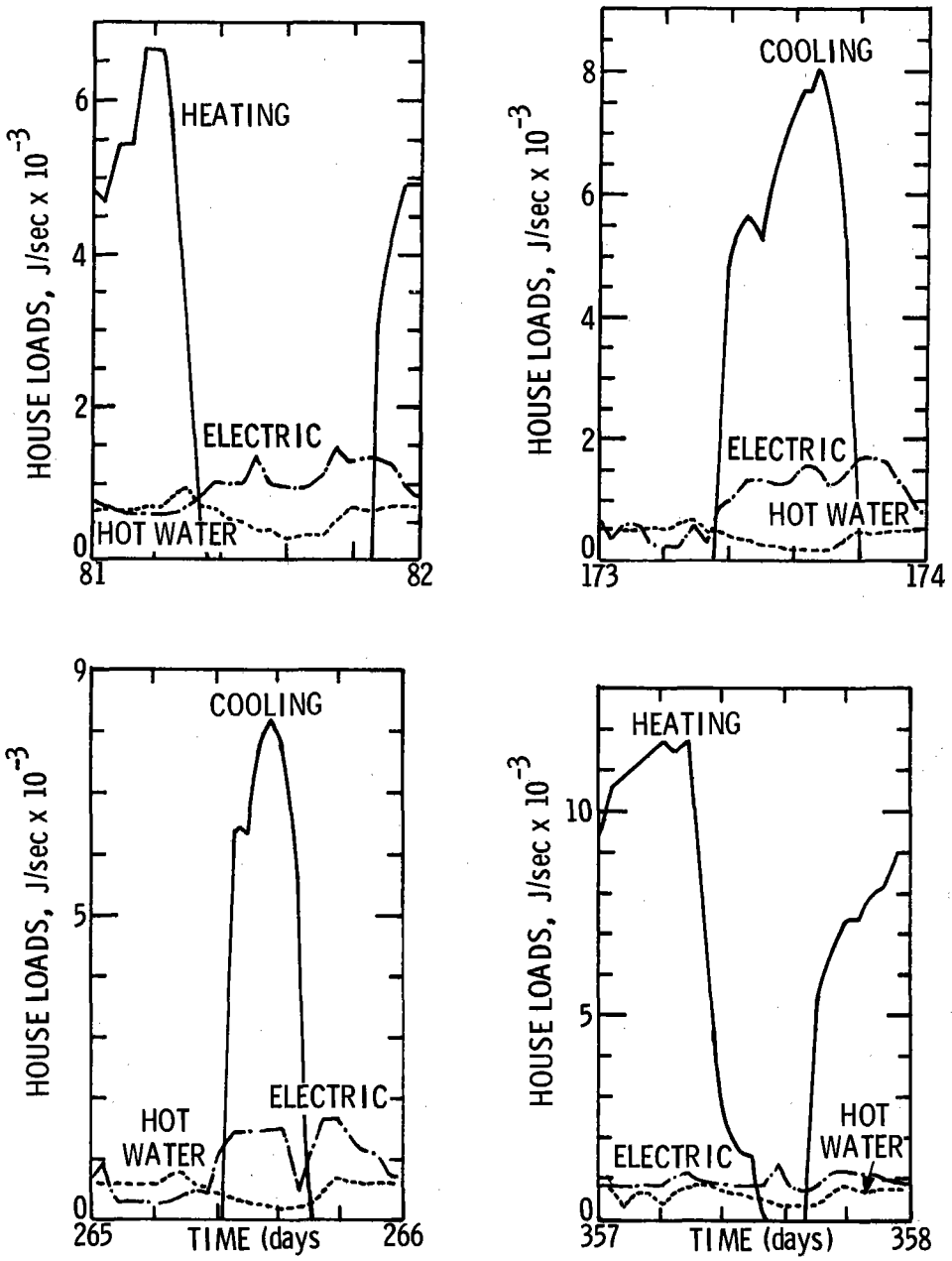

Figure 36. Electrical and thermal loads for a home located in Albuquerque

respectively. The overall efficiency was 17.9 percent and the temperature drop across the high-temperature storage system was 90°C (162°F). The cooling water was transmitted from the condenser to low-temperature storage at 88°C (190°F).

Figure 37 presents the response of the high- and low-temperature storage systems for a collector area of 24,230 m^2 which is equivalent to 17.5 percent of the total home roof area. The storage was sized to provide energy for overnight operation, and overcast days were not included. In all seasons except winter, 1400 m^3 (49,400 ft^3) of high-temperature storage is adequate to provide overnight operation. The low-temperature storage system cycles daily in both summer and winter; this results in significant fossil fuel consumption. During winter, low-temperature energy storage is depleted overnight for heating; during summer, it is depleted during the day for cooling. Fourteen hundred m^3 (49,400 ft^3) of low-temperature storage is required.

Figure 38 shows the operation of the two auxiliary fossil-fuel systems. These furnaces operate at times when the corresponding storage systems are depleted. During spring, the high-temperature furnace operates once just prior to solar insolation, whereas the low-temperature furnace does not operate because storage is adequate. During summer and fall, the high-temperature system does not operate, whereas the low-temperature system operates to augment the depleted storage system in meeting the cooling load. During winter, both systems operate; the low-temperature system operates extensively during the night to satisfy the high heating demands.

Figure 39 shows the operation of both cooling towers. In the spring, both operate when the storage systems are filled because the loads are less than those which occur during other seasons. During summer and fall, the high-temperature tower operates for a very limited time; during winter, neither tower operates because of the higher winter loads. Throughout the year, approximated by the 16-day sample, less than 4 percent of the energy collected is dissipated in the cooling towers.

Figures 37, 38, and 39 illustrate the seasonal variation in the operation of the system. The criterion in this design is that minimal solar energy be dissipated in the cooling towers. The storage capacity is sized for overnight use, and the stored energy cycles daily throughout most of the year. In addition, fossil fuel consumption is minimized.

The question of how much of the community energy requirements are satisfied by solar energy can be estimated by averaging the solar and fossil fuel use for the four seasons as represented by the 16 days. The solar outputs for spring, summer, fall, and winter are 522, 578, 507, and 400 GJ/day, respectively. Fossil fuel use is 91, 158, 260, and 550 GJ/day for the corresponding seasons. Thus, on a yearly basis, solar energy based on clear-day solar intensities provides 73 percent of the requirements. Cloudy days will obviously reduce this ratio, and solar data which will include cloud effects will be included in the analysis when they become available.

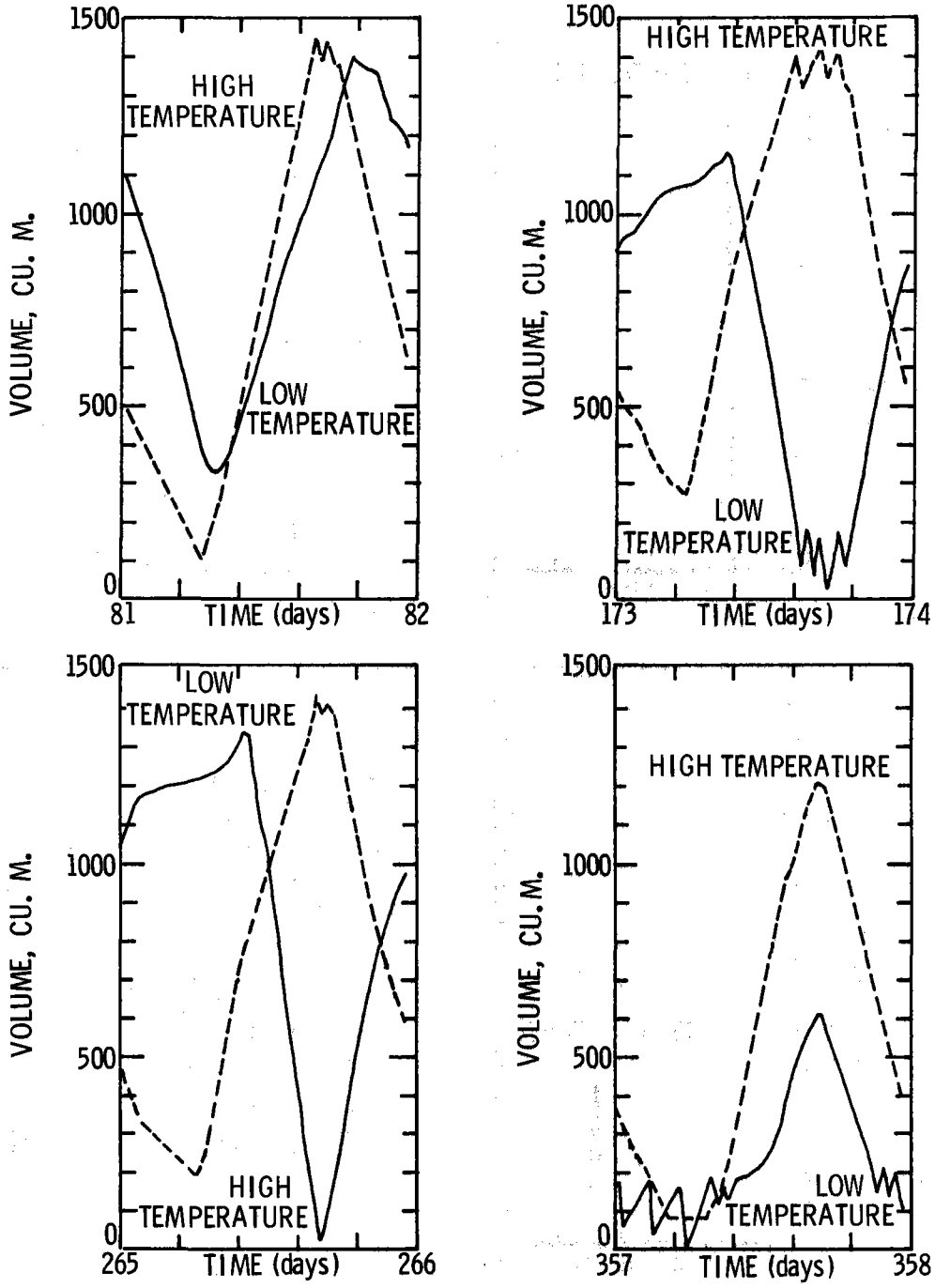

Figure 37. Storage response for overnight storage for a 1000-home community in Albuquerque

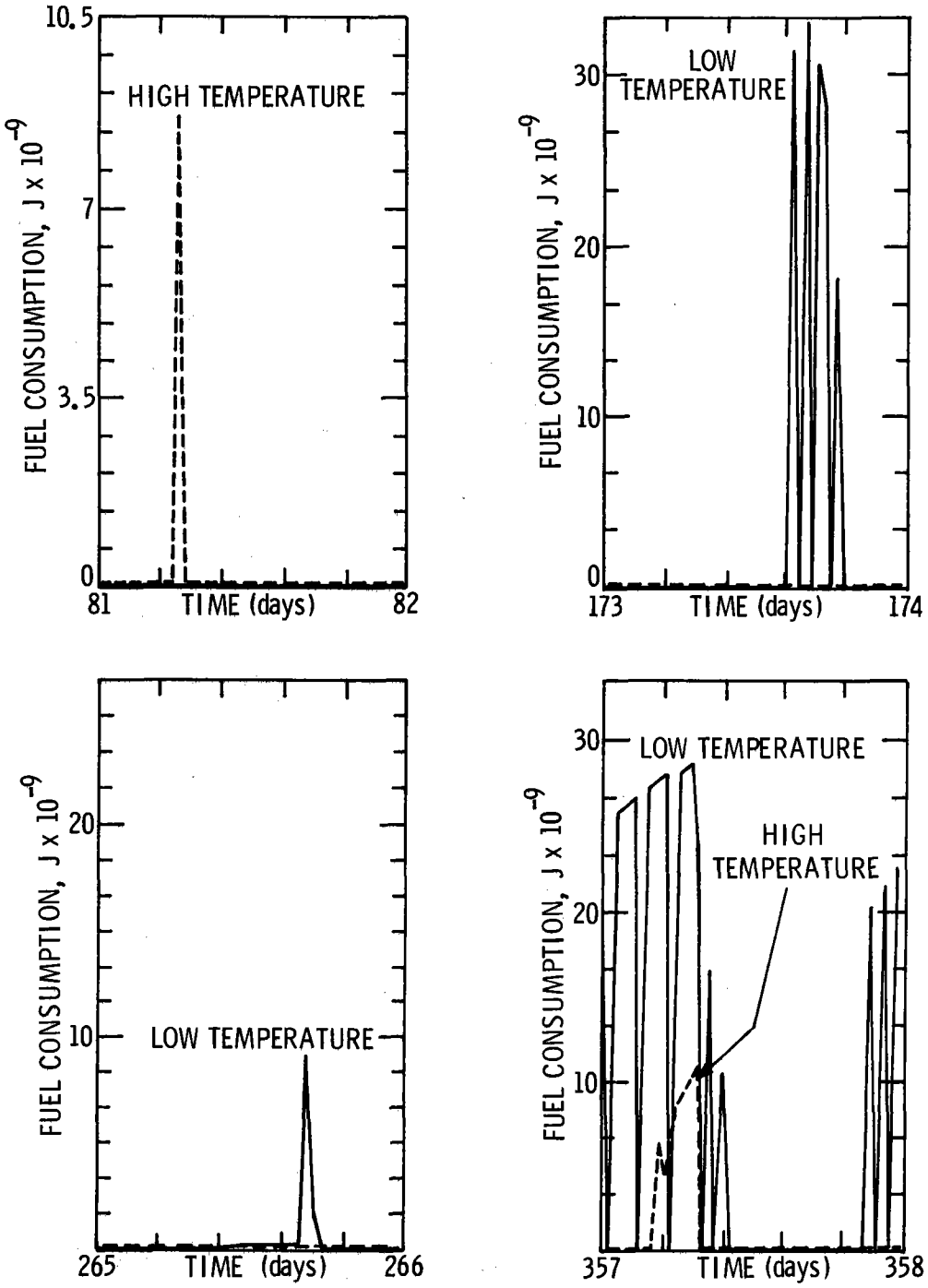

Figure 38. Fossil fuel consumed in auxiliary furnaces for a 1000-home community in Albuquerque

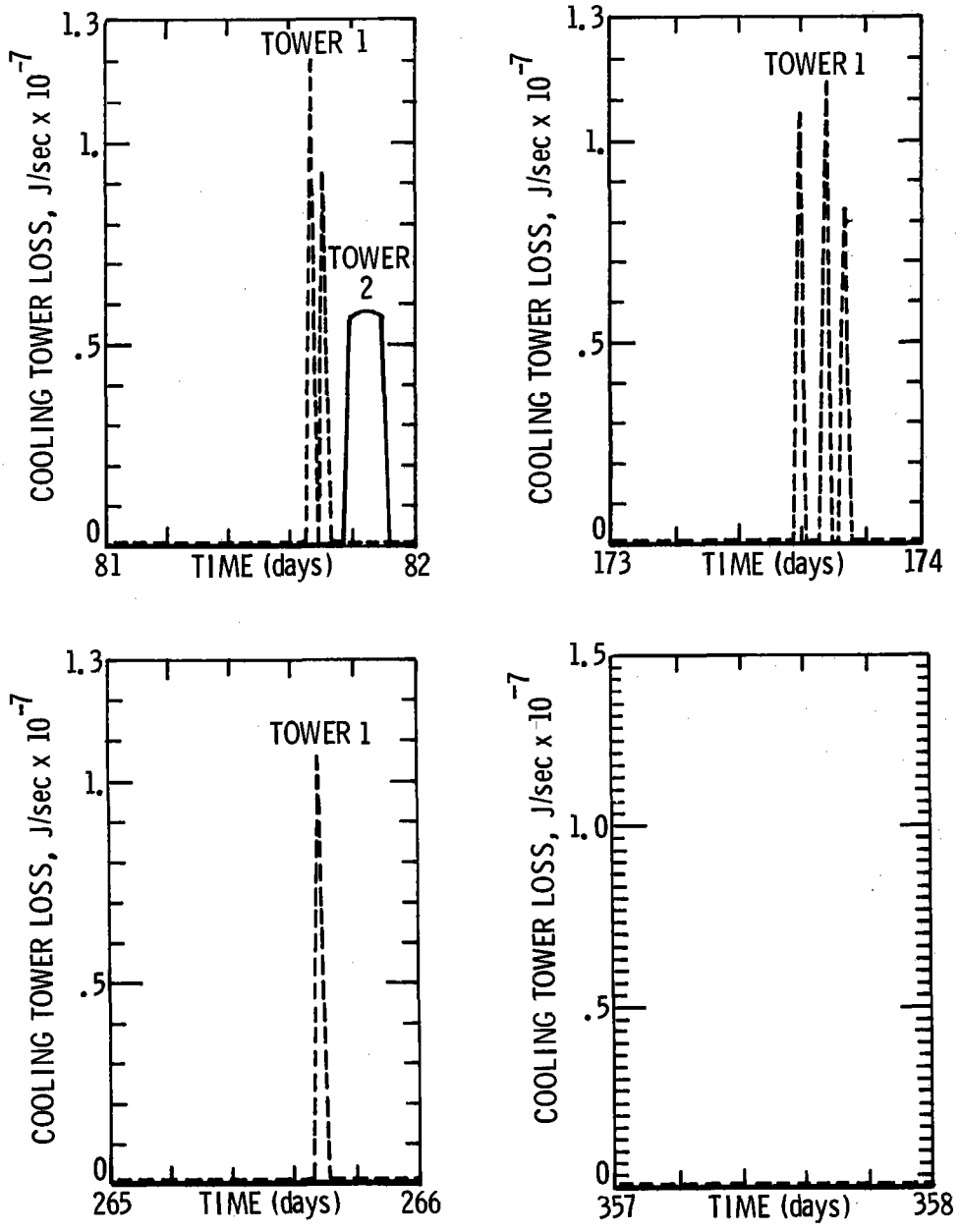

Figure 39. Energy dissipated in cooling towers for a 1000-home community in Albuquerque

Different total collector areas obviously can be used to provide energy for the community. However, larger collector areas will require either additional storage or more energy dissipation in the cooling towers. Likewise, smaller areas will require more fossil fuel. Systems which include a range of collector areas are presently being studied. Also, collectors mounted horizontally in an east-west direction are being studied as are systems with no high-temperature storage capacity. Results from those studies will be presented in future reports.

In comparing various total energy systems, an argument can be made for utilization of a low-temperature noncascaded total energy system. The cost factors that tend to make this approach attractive are (1) low-cost flat-plate collectors capable of utilizing diffuse as well as direct radiation and (2) lower temperature sensible heat storage allowing the use of water instead of high-priced heat transfer fluids.

A noncascaded total energy system utilizing a low-temperature Rankine cycle, 149°C (300°F) flat-plate collectors, pressurized water storage for Rankine-cycle energy storage, and unpressurized water for thermal energy storage is being compared on an economic basis to the 315°C (600°F) cascaded system currently under development. Preliminary results indicate near economic parity between the two systems. Consequently, such a system may be a viable competitive alternate.

Task 9.1 - Collector Fabrication Development

Alternate Trough Development. In addition to the contour forming approach, several other techniques are being investigated for fabricating 2.74- x 3.66-m troughs.

The two N/S reflectors produced by the MFG Boat Company have demonstrated the basic capability of utilizing boat hull technology to produce parabolic troughs of reasonable accuracy. The environmental and reflector performance capabilities of these two units will be monitored over the next several months. Although no other units of this type are presently planned, the experience of fabrication indicated several means of improving both the design and the process so that the cost of future units could be reduced. This potential will be evaluated against the cost and performance of the low cost units.

A spray-up process which sprays chopped fiberglass and polyester resin simultaneously has been used to fabricate a quarter-section of a 2.74- x 3.66-m reflector. This quarter-section will also be evaluated from environmental, cost, and accuracy viewpoints.

A third fabrication technique for large troughs based on circular architectural roof arches of large size and radii is being evaluated. Roof sections with radii of 2 to 6 meters are standard. This approach is very similar to the original trough design which used metal honeycomb and stressed fiberglass/epoxy skins. The roof arches use 1/4- or 3/8-inch flat plywood as the stressed skin and one of several inexpensive core materials in lieu of metal honeycomb; these include paper

honeycomb, additional solid plywood, rigid foam, and curved wooden spacer beams or ribs. The very large skins are produced by joining standard flat plywood sheets with butt or scarf joints. Although this concept is being investigated, it presents several major problems. Architectural arches do not normally meet the tight contour tolerances required for a good parabolic reflector. Second, the tensile strength of the plywood (with joints) is so low that there may be no advantage in going to a stress-skin structure for which a major structural support frame would still be required. The labor and materials of a sandwich structure, even a one-piece 10-m^2 unit, would be more costly than that for the four smaller contour molded piece produced in a high-volume production process.

Attempts are being made to locate a source and/or process by which the entire 2.74- x 3.66-m trough can be fabricated as one piece rather than in four sections; thus far, the right combination of press size, capacity, throat opening, and heating capability has not been found. Variations on these design and materials approaches are being pursued in a continuing effort to simplify the design and reduce the costs of fielding focusing reflector troughs.

Alternate Reflector Materials. Reflector materials development is an area where notable improvement in reflectance or decreases in cost could pay important dividends. Figure 40 illustrates the gains and losses from a collector as a function of operating temperature. Through the use of a glass vacuum-jacket, the convection and radiation losses have been substantially lowered. The greatest potential for improvement is in increased mirror reflectivity.

Reflector materials which are under evaluation as an alternative to Alzak include: silvered glass (common mirrors), acrylic sheet with evaporated silver and aluminum on either front or rear surface; various aluminum foils; Tedlar, Mylar, and Teflon films with back-surface evaporated aluminum or silver; and combinations of some of these films.

Samples of many reflector materials have been obtained from various manufacturers. Measurements of near-normal solar reflectance have been made in an integrating sphere reflectometer. These measurements have given some indication of the relative potential of the various materials, but specular reflectance data are absolutely indispensable to the selection of a reflector for a focusing collector. A goniophotometer, which measures reflectivity as a function of wavelength, incidence angle, and solid aperture angle, is now in use.

Humidity and thermal cycling tests are being conducted on many of the reflector samples to determine their resistance to the degradation associated with the environment. The thermal cycle test conditions are three cycles per day between -20° F and +130° F.

Sagged Glass Mirrors. A purchase order has been placed for delivery in October 1974 of eight each 60- x 160-cm (24- x 62.6-in.) glass sheets which have been sagged to parabolic contour to fit the large troughs. Sandia's glass shop will apply silver and protective paint coatings on these

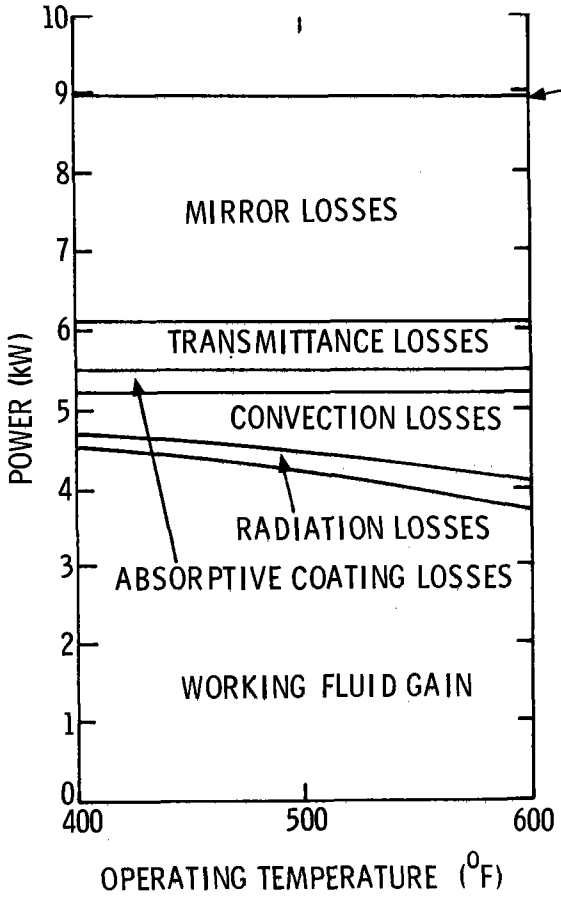

Collector power losses

sheets for evaluation and test. These silvered glass units can be bonded or mechanically attached to a full-sized trough for full-scale testing. Samples of silvered glass mirrors with various standard industrial protective paint coatings have been undergoing testing to determine temperature stability.

Task 9.2 - Storage Technology

Preliminary investigations into the possibility of flywheel energy storage are continuing. A flywheel has a potential advantage over sensible heat storage because the energy is stored after the efficiency losses of the turbine thermodynamic cycle have been incurred; the flywheel system therefore requires much less storage capacity. The tradeoff then becomes the increased cost of storage versus the decreased amount of storage required.

Presently, three significant problems are associated with flywheel energy storage. First, in order to keep bearing friction losses down to acceptable levels, the energy wheel must be supported on magnetic bearings. Second, to make efficient use of material, flywheel speeds must be high. This will require operation in a partial vacuum to minimize windage losses. Third, energy must be imparted to the wheel and extracted from it by some efficient means.

An investigation into the state of the art for flywheel energy storage has been conducted. As a consequence, it is felt that workable solutions exist for low-friction support of a high-speed wheel, problem one and two above. However, present input/extraction efficiencies of the order of 75 percent for small wheels are not sufficient to make flywheel storage economically competitive with sensible heat. Other methods of input/extraction are currently being investigated to determine whether improvements in this efficiency are possible.

Task 10 - Coatings Evaluation

Electrodeposited black chromium has promise as a selective absorber coating for receivers. Coatings with high solar absorptance (α_s = 0.95) and relatively low emittance (ϵ = 0.27 at 300°C) have been obtained. Preliminary studies indicate good stability at temperatures of 300-400°C in a vacuum environment.

Studies are now being directed toward obtaining the combinations of film thickness and substrate surface finish to give optimum values of α_s and ϵ. It has been found that α_s can be increased without significantly increasing emittance by increasing substrate roughness from a bright, highly polished nickel-plated surface to a matte or dull finish. The extent to which emittance can be reduced (without materially alterning α_s) by depositing a thin layer of low-emissivity material such as gold between the substrate and the electrodeposited black chrome is also being investigated.

The use of surface roughness to increase the solar absorptivity of vacuum-deposited semiconductor films is also being investigated. It has been found that vacuum-deposited thin films

(0.5 μm) of lead sulfide (PbS) have an $\alpha_s = 0.98$ and $\epsilon_{240°C} = 0.2$. This is attributed to the inherent rough surface morphology found in these vacuum-deposited thin films. These PbS films are stable at high temperatures in vacuum.

Thin films (0.5 μm) of germanium have been prepared by "gas evaporation" techniques. These films have a high absorptivity and a low emissivity ($\alpha_s = 0.91$, $\epsilon_{240°C} = 0.2$) but are not stable on heating in vacuum. Thicker germanium films (1 μm) which have a higher emissivity ($\alpha_s = 0.98$, $\epsilon_{240°C} = 0.48$) are stable on exposure to high temperatures in a vacuum.

Task 11 - Technology Utilization

A report describing the Solar Test Facility and its capabilities is in publication. This report will function as a test planning and user's guide document which will be available to future users of the facility.

The Collector Test Facility was made available for two days in July to Corning Glass Company personnel for testing of the Corning multitube-type solar collectors. Test planning, data taping, and data reduction were performed by Corning personnel.

DISTRIBUTION:

A. Warren Adam
Sundstrand Electric Power
4747 Harrison Avenue
Rockford, Illinois 61101

J. D. Balcomb
Los Alamos Scientific Lab
Assistant Division Leader
for Analysis & Planning
Mail Stop 571
Los Alamos, NM 87544

Richard Balzhizer
Office of Science & Technology
Executive Office of the President
Washington, D. C. 20506

Barber-Nichols Engineering
6325 West 55th Avenue
Arvada, Colorado 80002

Charles D. Beach
Westinghouse Georesearch Laboratory
8401 Baseline Road
Boulder, Colorado 80303

Jerry O. Bradley
Midwest Research Institute
425 Volker Blvd.
Kansas City, Missouri 64110

Floyd Blake
Martin Marietta Aerospace
Denver Division
P. O. Box 179
Denver, Colorado 80201

Karl W. Boer
Institute of Energy Conversion
University of Deleware
Newark, Deleware 19711

P. B. Bos
Manager, Solar Projects
Energy Projects Group
P. O. Box 92957
Aerospace Corporation
Los Angeles, California 90045

James C. Bresee
E463
Division of Applied Technology
Atomic Energy Commission
Germantown, Maryland 20767

Harold Bullis
Science Policy Division
Congressional Research Service
Library of Congress
Washington, D. C. 20540

J. O. Carnes
Southern Union Gas Company
Fidelity Union Tower Building
Room 1537
1507 Pacific Avenue
Dallas, Texas 75201

Ronal Larsen
Office of Technology Assessment
Old Immigration Building, Rm. 722
119 D St., NE
Washington, D. C. 20002

Commanding General
White Sands Missile Range
Attn: STEWS-TE-NT
Marvin Squires
White Sands Missile Range, NM 88002

John Martin
Argonne National Laboratory
9700 S. Cass Ave.
Argonne, Ill., 60439

J. R. Cotton, Chief
Reimbursable Activities Branch
USAEC/ALO
Albuquerque, NM 87115

Joe Guthrie
Enviro-Dynamics
3700 McKinney Ave.
Dallas, Texas 75204

B. D. Daugherty
Southern Union Gas Company
8th and Silver SW
Albuquerque, NM 87103

Jesse C. Denton
National Center for Energy
Management and Power
113 Towne Building
University of Pennsylvania
Philadelphia, Pennsylvania 19104

Gus Dorough
Deputy Director for Research & Advanced
Technology
Room 3E144/Pentagon Mail Stop 103
Washington, D. C. 20540

Solar Energy Application Lab.
Colorado State University
Ft. Collins, Colorado 80521

H. Silha
University of Idaho
Moscoe, Idaho 83843

DISTRIBUTION: (cont.)

Lou Werner
Division of Applied Technology
Atomic Energy Commission, HQ
Germantown, Maryland 20767

Frank Zarb
Office of Management and Budget
Washington, D.C.

Sam Taylor
Federal Energy Administration
Washington, D. C.

Louis O. Elsaesser
Director of Research
Edison Electric Institute
90 Park Avenue
New York, New York 10016

Edward H. Fleming
Room E-479
Division of Applied Technology
Atomic Energy Commission
Germantown, Maryland 20767

Richard Hill
Federal Power Commission
441 G. Street, N. W. Room 4005
Washington, D. C. 20426

George Kaplan (10)
National Science Foundation
1800 G. Street, N. W.
Washington, D. C. 20550

Charles Kelber
Argonne National Laboratory
9700 South Cass Avenue
Argonne, Illinois 60439

D. K. Nowlin, Director
Special Programs Division
U.S. Atomic Energy Commission
Albuquerque, NM 87115

Martin Prochnik
Deputy to the Science Advisor
U.S. Department of Interior
Room 5204
Washington, D. C. 20204

James E. Rannels (20)
Division of Applied Technology
Atomic Energy Commission, HQ
Germantown, Maryland 20767

M. W. Rosenthal
Oak Ridge National Laboratory
P. O. Box Y
Oak Ridge, Tennessee 37830

R. San Martin
New Mexico State Univeristy
Las Cruces, NM 88001

R. Schmidt
Systems & Research Center
Honeywell Incorporated
2700 Ridgeway Road
Minneapolis, Minnesota 55413

G. Schreiber
Publich Service Company
414 Silver Avenue, SW
Albuquerque, NM 87103

J. W. Schroer, Chief
Special Projects Branch
USAEC/ALO
Albuquerque, NM 87115

Robert W. Scott
Manager, USAEC/SAO
Albuquerque, NM 87115

Alan R. Siegel
Director, Environmental Factors & Public
Utilities Division
Department of Housing & Urban Development
Washington, D. C. 20410

F. M. Smits
Bell Laboratories
555 Union Boulevard
Allentown, Pennsylvania 18103

Dwain Spencer (5)
Electric Power Research Institute
3412 Hillview Avenue
Palo Alto, California 94304

Ross Stickley
G.T.S. Sheldahl Company
Northfield, Minnesota 55057

Pete Susey
American Gas Association
1515 Wilson Boulevard
Arlington, Virginia 22209

Ira Thierer
Southern California Edison
P. O. Box 800
2244 Walnut Grove Avenue
Rosemead, California 91770

U.S. Atomic Energy Commission
Division of Military Application
Attn: Major Gen. Frank A. Camm
Asst. Gen. Manager for Military
Application
Washington, D. C. 20545

DISTRIBUTION: (cont.)

Lorin L. Vant-Hull
Department of Physics
University of Houston
3801 Cullen Boulevard
Houston, Texas 77004

Michael Wahlig
Lawrence Berkeley Laboratory
Building 50A, Room 6121
University of California
Berkeley, California 94720

W. A. Cross
Attn: M. Wilden
Department Mechanical Engineering
University of New Mexico
Albuquerque, NM 87106

Karl Willenbrock
Director, Institute for Applied Technology
National Bureau of Standards
Room B-112 - Tech (400.00)
Washington, D. C. 20234

Leonard S. Raymond
Optical Sciences Center
Tucson, Arizona 85721

Samuel J. Taylor
Federal Energy Administration
Solar Energy Office
Room 3443
1200 Pennsylvania Ave NW
Washington, DC 20461

1100 C. D. Broyles, Attn: 1110 J. D. Kennedy
1120 G. E. Hansche

1540 T. B. Lane, Attn: 1543 H. C. Hardee
2300 L. D. Smith
2320 K. Gillespie, Attn: 2324 L. W. Schulz
2400 R. S. Claassen
2440 O. M. Stuetzer, Attn: 2441 G. W. Gobeli
4700 D. B. Shuster
4730 R. G. Clem, Attn: 4734 V. L. Dugan
5000 A. Narath, Attn: 5100 J. K. Galt
5200 E. H. Beckner
5600 A. Y. Pope
5110 F. L. Vook
5130 G. A. Samara
5150 J. E. Schirber
5220 J. V. Walker, Attn: 5223 J. H. Renken
5620 R. C. Maydew
5700 J. H. Scott, Attn: 5720 M. L. Kramm
5710 G. E. Brandvold, Attn: 5716 W. N. Caudle
5712 R. H. Braasch (50)
5717 R. P. Stromberg (25)
5718 M. M. Newsom
5800 L. M. Berry, Attn: 5820 R. L. Schwoebel
5830 M. J. Davis, Attn: 5834 D. M. Mattox
5840 D. M. Schuster, Attn: 5842 R. C. Heckman
5844 F. P. Gerstle
5846 E. K. Beauchamp
8100 L. Gutierrez
8180 C. S. Selvage, Attn: 8184 A. C. Skinrood
9300 L. J. Paddison
9330 A. J. Clark, Jr. Attn: 9331 P. H. Adams
9340 W. E. Caldes, Attn: 9344 E. R. Julius
9400 L. A. Hopkins
9410 R. L. Brin, Attn: 9412 R. K. Petersen
9474 L. W. Scully
9700 R. E. Hopper, Attn: 9740 H. H. Pastorius
9750 R. W. Hunnicutt
3141 L. S. Ostrander (5)
8266 E. A. Aas (2)
3151 W. F. Carstens (3)
for AEC/TIC (Unlimited Release)
6011 G. C. Newlin

Org.	Bldg.	Name	Rec'd by*	Org.	Bldg.	Name	Rec'd by*

*Recipient must initial on classified documents.